CHAPTER 6

Structural and metamorphic evolution of the central Arunta Block: a synthesis

Summary

The central Arunta Block is interpreted to have undergone two major tectonometamorphic cycles during the early- to mid-Proterozoic. On the basis of regional correlations, these cycles appear to have affected a large portion of the Arunta Block. The early- to mid-Proterozoic tectonic evolution of the central Arunta Block is inferred to have involved: (1) asymmetrical lithospheric extension and concomitant crustal thickening due to magmatic accretion, which resulted in peak metamorphic conditions; (2) thermal relaxation and ductile non-coaxial extension along a northeast-southwest tectonic axis; (3) crust/mantle delamination, which resulted in rising of the asthenosphere and gravitational instabilities in the crust; (4) crustal shortening and thickening followed by limited crustal thinning related to gravitational collapse; and (5) isobaric cooling at depth until uplift and exposure at the surface in the late-Proterozoic and/or mid-Carboniferous.

6.1 Introduction

Evidence for the structural and metamorphic evolution of the central Arunta Block is provided by the structure and alignment of minerals in kinematic fabrics from rocks in the Strangways Metamorphic Complex, Harts Range Group and numerous shear zones that dissect the terrain. Together with the regional geological history, the structural and metamorphic evolution provide a basis for deriving a tectonic model for the evolution of the central Arunta Block and inferring the processes that may have been responsible for deformation and metamorphism.

Five deformations (D_1-D_5) and two metamorphisms (M_1-M_2) have been recognized in rocks from the Strangways Metamorphic Complex. D_1-D_2 occurred during an early deformation cycle associated with peak metamorphism (M_1, Chapter 2). D_3-D_5 occurred during a progressive, regional, compressive deformation associated with an increase in temperature and pressure during M_2 (Chapters 3 and 4).

Deposition of the Reynolds Range Group (Dirks and Norman, 1991; Appendix) occurred at about the same time as D_1-D_2 (1800 Ma) in the Strangways Metamorphic Complex on a shallow southwest-dipping marine shelf. The geometry of the shelf and coastline may have been influenced by the deformation and metamorphic processes in the central Arunta Block.

The inferred early-Proterozoic P-T-(t) path for rocks of the Harts Range Group is different from that inferred for rocks in the Strangways Metamorphic Complex. This may reflect a different stratigraphic and structural setting for the Harts Range Group. In this Chapter, the structure of the Harts Range Group, which is similar to the structure of large parts of the Arunta Block, is described. The structural and metamorphic history of shear zones that separate the Strangways Metamorphic Complex and the Harts Range Group is also discussed. Deformation structures in gneisses adjacent to the Amadeus Basin and in the late-Proterozoic Heavitree Quartzite are also briefly described, in order to

delineate the effects of the mid-Carboniferous Alice Springs Orogeny, which was responsible for intense deformation along the northern margin of the Amadeus Basin.

6.2 Structural and metamorphic evolution of the Strangways Metamorphic Complex

6.21 Ongeva granulites and the Anamarra granite domain

Part of the tectonometamorphic evolution of the Ongeva granulites and the Anamarra granite domain has been attributed to two major deformation cycles (Chapter 2) and two associated metamorphisms (Chapter 3). Deformation during the first deformation cycle (D_1-D_2) was accompanied by anatexis due to peak metamorphism (M_1), the deformation and crystallization of S_2 leucosome having occurred during D_2. S_2 is oriented subparallel to the lithological layering and could have been initially recumbent. U-Pb zircon data indicate D_2 to have occurred at 1765±4 Ma (Norman and Collins, unpublished data) and peak metamorphism is inferred to have occurred at about 1800 Ma (Black et al., 1983; Windrum and McCulloch, 1986). There appears to be no large-scale repetition of "stratigraphy" associated with D_1 nor D_2, and M_1 and S_2 mineral assemblages indicate that peak metamorphism was followed by limited decompression with cooling (Chapters 3 and 4). However, the D_2 structures indicate extreme extension, which was probably associated with large simple-shear strain accumulations. Peak metamorphism involved perturbation of the geotherm and was accompanied by a high surface heat flux of at least $100mWm^{-2}$ (after Bohlen, 1991). Evidence for a high geothermal gradient in Proterozoic terrains has been attributed to magmatic heating (Oxburgh and Turcotte, 1970; England and Thompson, 1986; Bohlen, 1991) contemporaneous with crustal and lithospheric thinning (McKenzie, 1978; Wickham and Oxburgh, 1985; Sandiford and Powell, 1986). Layer-parallel foliations are inferred to have accompanied prograde metamorphism during compressional (Bohlen, 1987; Clarke et al., 1987; Hobbs et al; 1984) or extensional (Sandiford, 1989) deformation. Structural and metamorphic fabrics from the Ongeva granulites and the Anamarra granite domain indicate that limited crustal thickening occurred during M_1/D_1 and that

development of a layer-parallel foliation occurred primarily after peak metamorphism during intense ductile non-coaxial extensional deformation. There is no evidence that crustal thickening during M_1 was associated with compressional tectonic structures; it is inferred as having been due to magmatic overaccretion and underplating. Massive granitoids intruded low-pressure terrains elsewhere in the Arunta Block at the same time as peak metamorphism (M_1) and D_2 deformation in the Strangways Metamorphic Complex (1800-1760 Ma, Collins et al., 1991). Inferred decompression for the Strangways Metamorphic Complex can be related to isostatic compensation of the lithosphere, which is expected when large volumes of felsic magma are added to the crust (e.g. Thompson and Ridley, 1987; Stüwe and Powell, 1989a, 1989b). The M_1 P-T path inferred for the Strangways Metamorphic Complex increases in pressure and temperature during the prograde metamorphic path and decreases slightly in pressure during slow cooling. This outlines a predicted anticlockwise path for mid-crustal terrains below a zone of magmatic accretion (Bohlen, 1991; Harley, 1989).

Although magmatic intrusion into the upper and lower crust helps to transfer heat from the mantle lithosphere, it may only be a consequence of an asthenospheric perturbation, such as lithospheric thinning (Wernicke, 1985). As noted by Sandiford and Powell (1986), maximum crustal extension may be asymmetrical with respect to maximum lithospheric thinning and maximum surficial heat flow. The deposition of supracrustal rocks in areas of maximum crustal extension during lithospheric thinning places constraints on the geometry of large-scale shear zones (detachments), which may be associated with extension. The recognition of a lateral metamorphic gradient during peak metamorphism also places constraints on the geometry of the extensional system, because the geothermal gradient decreases away form the area of maximum lithospheric extension. Later in this Chapter, inferred P-T-t paths, geothermal gradients and the geometry of supracrustal deposition are used to derive a tectonic model for the early evolution of the central Arunta Block involving crustal thickening and lithospheric thinning.

The similar orientation of structural fabric elements during D_3-D_5 suggests that they were produced during a continuous progressive deformational cycle. This is shown by the superimposed mean structural elements from the Ongeva granulites and the Anamarra granite domain in Fig. 6.1. The second deformation cycle was responsible for the complex fold pattern (D_3) and shear zone deformation (D_4-D_5) and has been termed the *Arunta Orogeny* (Chapter 2). The orientation of D_3 fold axes with respect to the stretching lineation indicates a probable northeast to southwest transport direction. The effects of a second metamorphic event (M_2) are recognized in the Strangways Metamorphic Complex by mineral assemblages that indicate an increase in temperature and pressure. M_2 was probably associated with compressional deformation during D_3-D_5. Intrusion of granite and metagabbro occurred after D_2 and may have been syntectonic with the early part of the second deformation cycle. U-Pb zircon data obtained from the Anamarra Granite indicate that intrusion of the igneous complex to have occurred at 1745±4 Ma (Norman and Collins, unpublished data). Therefore, D_3 is inferred to have occurred within 20 Ma of D_2 and 55 Ma of M_1. Metagabbro in the Anamarra granite domain is calc-alkaline and unlike tholeiitic, metabasic rocks that are interlayered with felsic rocks in the Ongeva granulites. Calc-alkaline igneous rocks are common in arc-type or collisional orogenic zones where oceanic crust is being consumed into the mantle (B-subduction). However, there are no high-pressure mineral assemblages nor obducted ophiolite in the Strangways Metamorphic Complex, which would indicate B-subduction. The intrusion of calc-alkaline plutons during D_3 was probably related to processes in the mantle lithosphere during cooling from peak metamorphism. Furthermore, D_3 deformation occurred in a shorter time than the thermal decay time for the continental lithosphere (England and Richardson, 1977; Loosveld and Etheridge, 1990) after D_1-D_2, and so could also be related to processes responsible for peak metamorphism. Mantle processes that could be responsible for granitoid intrusion and initiating the second deformation cycle are discussed later in this Chapter. Whole-rock compositions for the Anamarra Granite, metagabbro from the Anamarra granite domain and average mafic gneisses from the Ongeva granulites are

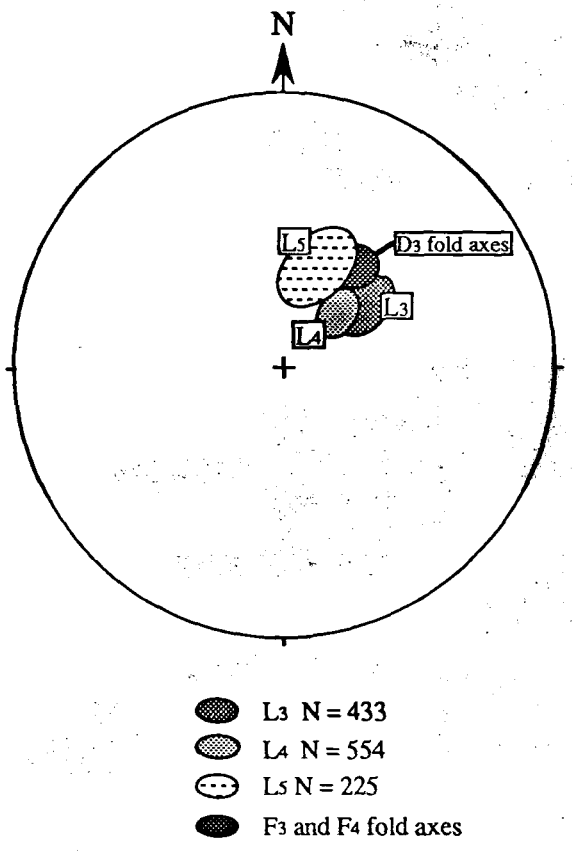

Fig. 6.1 Lower hemisphere, equal area, stereographic projections of L_3, D_3 fold axes, L_4 and L_5 from the Strangways Metamorphic Complex.

presented in Table 6.1. Coaxial shortening occurred during the later part of D_3 and was associated with lateral dextral shearing.

D_4 and D_5 deformation also occurred at granulite facies conditions and is characterized by ductile non-coaxial shear zones. D_4 shear zones could represent gravitational collapse due to crustal thickening during D_3 or may be antithetic to deformation between wide D_5 shear zones with reverse movement. However, the similar orientation of L_4 and L_5 stretching lineations in the shear zones and L_3 suggests that D_4 and D_5 are a continuation of the orogenic cycle responsible for D_3. They probably represent the partitioning of strain into localized zones, due to strain hardening and fluid channelling, as the terrain cooled during progressive compressional deformation. Cordierite-bearing metapelites that are deformed in D_5 shear zones in the Ongeva granulites contain a well-developed alignment of sillimanite and biotite (Fig. 6.2a) defining L_5, cordierite having been removed. Coarse-grained retrograde greenschist facies muscovite commonly occurs as random booklets, which contain sillimanite and biotite inclusions (Fig. 6.2b). Greenschist facies retrogression usually occurs near pegmatite dykes. Similar pegmatite dykes in the Harts Range have yielded a U-Pb zircon age of 520 Ma and a Rb-Sr muscovite age of 307 Ma (Mortimer et al., 1987). Metagabbro that is deformed by D_5 in the Anamarra granite domain contains porphyroblasts of anthophyllite and aligned hornblende (Fig. 6.2c), representing amphibolite facies retrogression in D_5 shear zones. In areas of greenschist retrogression within D_5 shear zones, hornblende is replaced by chlorite (Fig. 6.2d). Greenschist facies retrogression postdates high-grade D_5 deformation and amphibolite facies retrogression in the shear zones and is unrelated to the main penetrative structural and metamorphic fabrics in the Ongeva granulites and the Anamarra granite domain.

6.22 Structural and metamorphic fabrics in the Erontonga metamorphics and Ankala gneiss

The Erontonga metamorphics and the Ankala gneiss belong to the Strangways Metamorphic Complex and crop out between the Hale River and the deformed northern

Table 6.1 Whole-rock compositions from the Strangways Metamorphic Complex.

wt%	Anamarra Granite	metagabbro Anamarra granite domain	average mafic granofels Ongeva granulites
SiO_2	69.13	50.43	50.43
TiO_2	0.57	0.78	1.30
Al_2O_3	14.15	19.03	14.79
Fe_2O_3	1.18	2.16	3.22
FeO	2.68	7.71	8.21
MnO	0.05	0.18	0.13
MgO	0.84	5.46	7.24
CaO	2.68	10.17	10.57
Na_2O	2.01	3.26	2.21
K_2O	5.46	0.61	0.73
P_2O_4	0.14	0.05	0.14
H_2O+	0.98	1.44	0.55
H_2O-	0.17	0.12	0.05
CO_2	0.00	0.04	0.12
TOTAL	100.06	100.55	99.69
trace elements (ppm)			
Ba	1590	51	115
Ce			46
Cr	14	64	254
Cu	14	63	52
Ga	16	17	19
La			19
Nb	8	1	11
Nd			26
Ni	10	116	78
Pb	13	14	7
Pr			7
Rb	177	13	25
Sr	168	145	104
Th	5	0	2
U	0	0	2
V	34	175	244
Y	28	16	73
Zn	36	94	83
Zr	259	35	99

Fig. 6.2 (a) Garnet porphyroblasts and lineated sillimanite and biotite in a metapelitic schist on the northern margin of the Ongeva granulites. Sample 904. Base of photograph is 4.4 mm.

6.2 (b) Muscovite porphyroblast containing sillimanite and biotite inclusion trails in a sillimanite-biotite schist on the northern margin of the Ongeva granulites. Sample 901. Base of photograph is 2.0 mm.

6.2 (c) Hornblende-plagioclase metagabbro containing anthophyllite porphyroblasts. Anamarra granite domain. Sample 903A. Base of photograph is 4.4 mm.

6.2 (d) Chlorite schist containing anthophyllite porphyroblasts adjacent to sample in Fig. 6-2c in the Anamarra granite domain. Sample 903B. Base of photograph is 4.4 mm.

6.2 (e) Elongate staurolite defining a steep lineation in the Anuma schist.

6.2 (f) Lineated staurolite and biotite in the Anuma schist. Sample 945. Base of photograph is 4.4 mm.

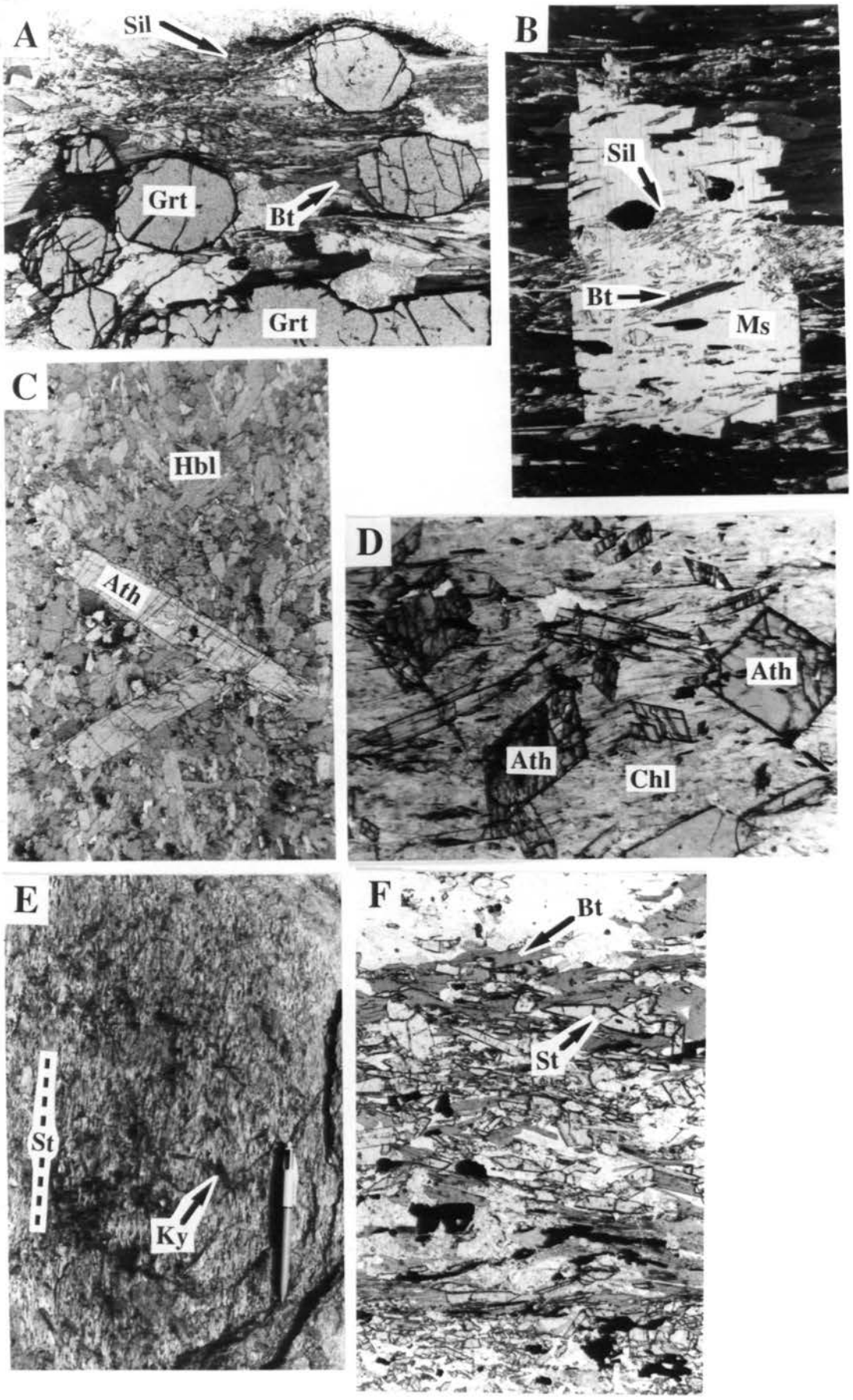
A
Sil
Grt
Bt
Grt
B
Sil
Bt
Ms
C
Hbl
Ath
D
Ath
Ath
Chl
E
St
Ky
F
Bt
St

margin of the Amadeus Basin (Figs 1.0, 1.1) in the Winnecke Block (Shaw and Langworthy, 1984). Although they are distinguished by different rock types elsewhere, no subdivision of these rock units are made in this study, due to intense deformation that transposed the compositional layers. The outcrop pattern of the Erontonga metamorphics and the Ankala gneiss in the Winnecke Gorge area is shown in Fig. 6.3 and structural data are presented on stereographic projections in Fig. 6.4.

The Erontonga metamorphics and the Ankala gneiss consist of quartzofeldspathic gneisses, mafic granulite facies gneisses, metapelitic gneisses and calc-silicate rocks. A gneissic tectonometamorphic foliation in the Erontonga metamorphics and Ankala gneiss is cut by a well-developed, pervasive north-dipping biotite foliation that contains a steep northeast-plunging stretching lineation (Fig. 6.4). A second foliation, defined by the alignment of biotite or medium-grained quartz and feldspar, is commonly oblique to the biotite foliation. The two foliations are typical of S-C planes in mylonites produced during non-coaxial deformation (Berthé et al., 1979; Lister and Snoke, 1984). The orientation of these fabrics preserves evidence of south-directed shearing. Asymmetrical feldspar augen are also common and preserve evidence of south-directed shearing. The original orientation of fabrics associated with the early gneissic foliation could not be determined, due to the intensity of recrystallization during later deformations, which rotated the early foliations into parallelism with the biotite foliations. The mylonitic foliation dips mostly 60° to the north, but is spread about a steep small-circle axis (Fig. 6.4). It has a similar distribution to the pervasive foliation in the Gough Dam Schist Zone (see Fig. 2.12). The plunge of mineral elongation lineations is mostly 50° towards 021-000 and is also very similar to that in the Gough Dam Schist Zone.

Greenschist facies retrogression is common, particularly near the late-Proterozoic Heavitree Quartzite, which belongs to the Amadeus Basin (Fig. 6.3). Deformation of the Amadeus Basin occurred during the mid-Carboniferous Alice Springs Orogeny and was associated with the development of south-verging nappes (Forman, 1971; Majoribanks, 1976). Adjacent to the Erontonga metamorphics and the Ankala gneiss,

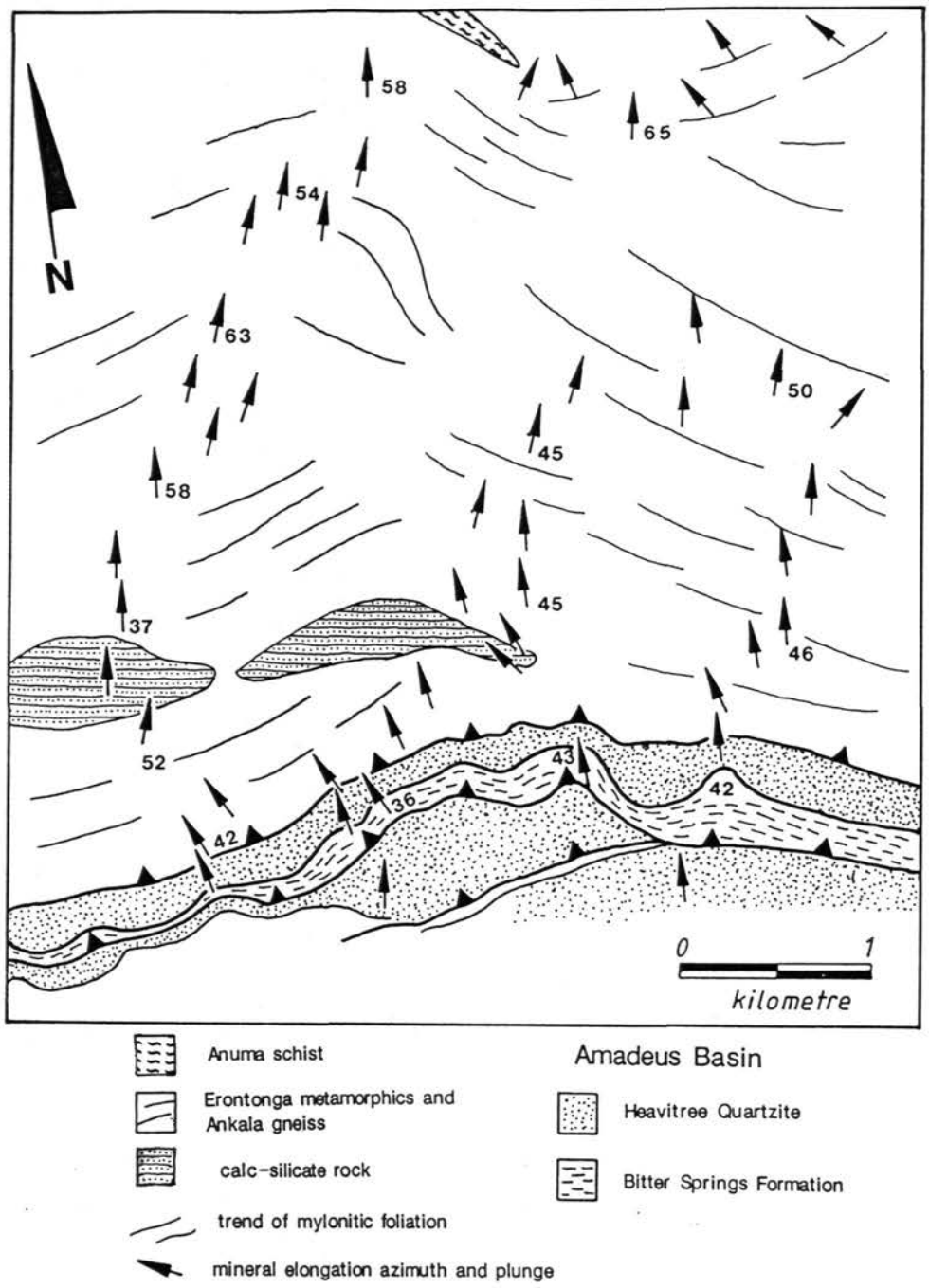

Fig. 6.3 Outcrop pattern of the Erontonga metamorphics, Ankala gneiss, Anuma Schist and late-Proterozoic Heavitree Quartzite. Location shown on Fig. 1-0.

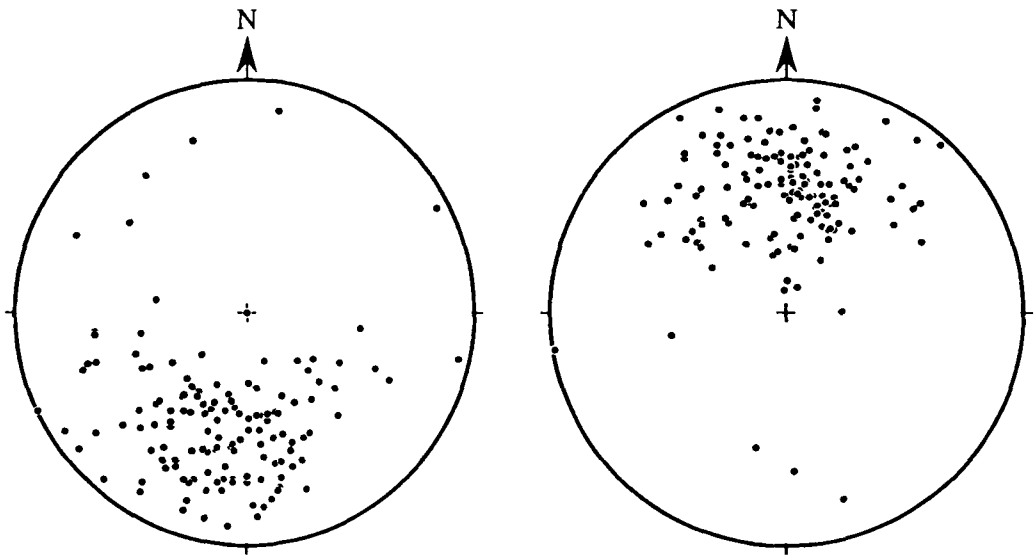

Poles to mylonitic foliations
N = 140

mylonitic lineations
N = 143

Fig. 6.4 Lower hemisphere, equal area, stereographic projections of poles to mylonitic foliations and mylonitic lineations from the Erontonga metamorphics and Ankala gneiss.

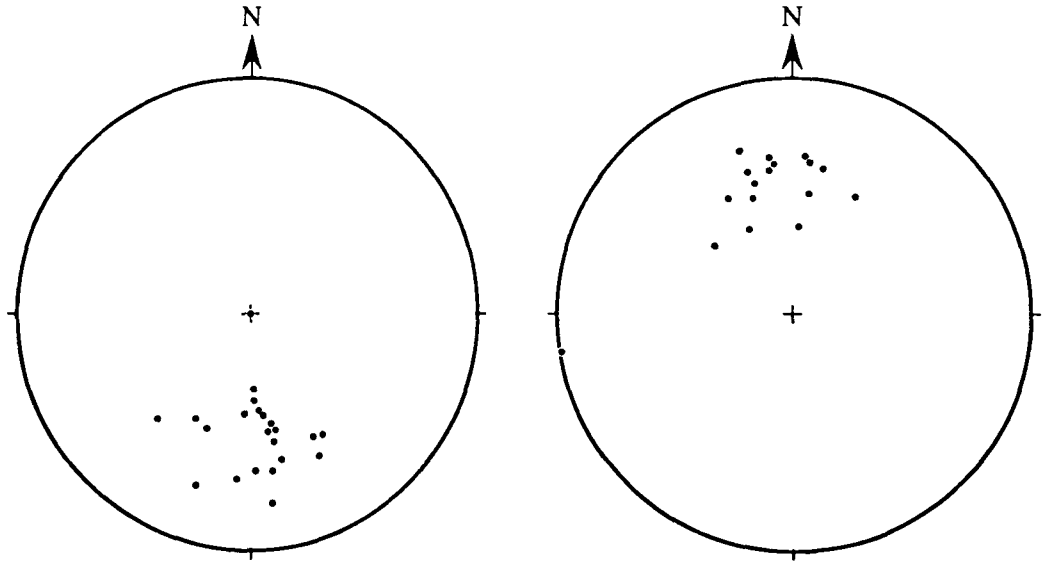

Poles to So in the Heavitree Quartzite
N = 22

Quartz elongation lineation in So
from the Heavitree Quartzite
N = 16

Fig. 6.5 Lower hemisphere, equal area, stereographic projections of poles to So from the Heavitree Quartzite and quartz elongation lineations on So.

the Heavitree Quartzite is recrystallized and contains a quartz elongation lineation. This lineation plunges between the northwest and the north (Fig. 6.5). In outcrops of the Erontonga metamorphics and the Ankala gneiss, north of the Heavitree Quartzite, an alignment of fine-grained white mica overprints the earlier mylonitic lineation. The later white mica lineation plunges to the northwest and is oblique to the earlier steep lineation. It is also subparallel to a quartz lineation in the Heavitree Quartzite, and is therefore correlated with deformation during the Alice Springs Orogeny. The distribution of L_5 and S_5 in the Gough Dam Schist Zone was attributed to D_5 deformation and post-D_5 crenulation (Chapter 2). Mylonitic deformation in the Erontonga metamorphics and the Ankala gneiss probably correlates with D_5 in the Gough Dam Schist Zone, which is part of the second deformation cycle in the Strangways Metamorphic Complex.

6.23 Structural and metamorphic fabrics in the Anuma schist

The Anuma schist is a coarse-grained biotite schist that contains staurolite, kyanite, sillimanite and fine-grained white mica. It crops out on the northern margin of the Erontonga metamorphics and the Ankala gneiss in the Winnecke Block (Shaw and Langworthy, 1984). The Anuma schist commonly contains a white-mica elongation lineation oblique to a steep high-grade mineral elongation lineation. The oblique white-mica lineation is subparallel to a similar lineation in the Erontonga metamorphics and Ankala gneiss adjacent to the Heavitree Quartzite, which is attributed to deformation during the Alice Springs Orogeny. Elongate staurolite and biotite are commonly aligned in a north-dipping biotite foliation and define a steep lineation in the Anuma Schist (Figs 6.2e, 6.2f). Lineated prisms of sillimanite similar to those in D_5 shear zones on the northern margin of the Ongeva granulites may also be aligned parallel to staurolite. Coarse-grained random kyanite may occur in pods or as porphyroblasts in the biotite foliation (Fig. 6.2e). Kyanite formation appears to postdate deformation as it is not lineated, and probably represents cooling into the kyanite stability field; this is the kyanite stage of Warren (1983a). Garnet was not found in the Anuma schist.

6.3 Structural and metamorphic history of the Harts Range Group

The Harts Range Group (Fig. 5.1) consists of folded, interlayered, garnet-bearing mafic gneisses, metapelitic gneisses, calc-silicate rocks and quartz-rich gneisses, which are cut by north-dipping mylonite zones that indicate a south-directed sense of shear. It crops out to the north of the White Lady Block, which consists of north-dipping shear zones and the Gough Dam Schist Zone. The White Lady Block and the Gough Dam Schist Zone separate the Harts Range Group from the Strangways Metamorphic Complex to the south. The Harts Range Group has been subdivided into the *Riddock Amphibolite Member*, *Irindina Gneiss* and the *Naringa Calcareous Member* (Shaw et al., 1984b). The Harts Range Group has also been subdivided into the Harts Range meta-igneous complex and Irindina supracrustal assemblage, on the basis of geochemical data (Sivell and Foden, 1985). However, in this Chapter the Harts Range Group is subdivided, following Shaw et al. (1984b), into a series of spatially distinct blocks that are separated by mylonite zones. Each block preserves a distinct structural history. The Irindina Gneiss crops out to the south of the Riddock Amphibolite Member and the Naringa Calcareous Member crops out to the north of the Riddock Amphibolite Member (Fig. 6.6). The outcrop pattern of the Harts Range Group is shown in Fig. 6.6.

6.31 Structural geology of the Riddock Amphibolite Member

The Riddock Amphibolite Member forms a large garnet-bearing, mafic sheet that is continuous for a distance of more than 60 km east of Mount Riddock. The Riddock Amphibolite Member is folded and contains minor interlayered garnet-bearing felsic gneisses and quartzites. Structural data from the Riddock Amphibolite Member are presented on stereographic projections in Fig. 6.7.

The Riddock Amphibolite Member contains a tectonometamorphic gneissic foliation (S_2) that is defined by cm-scale alternations of coarse-grained plagioclase-rich±garnet±amphibole leucosome and coarse-grained granoblastic layers of

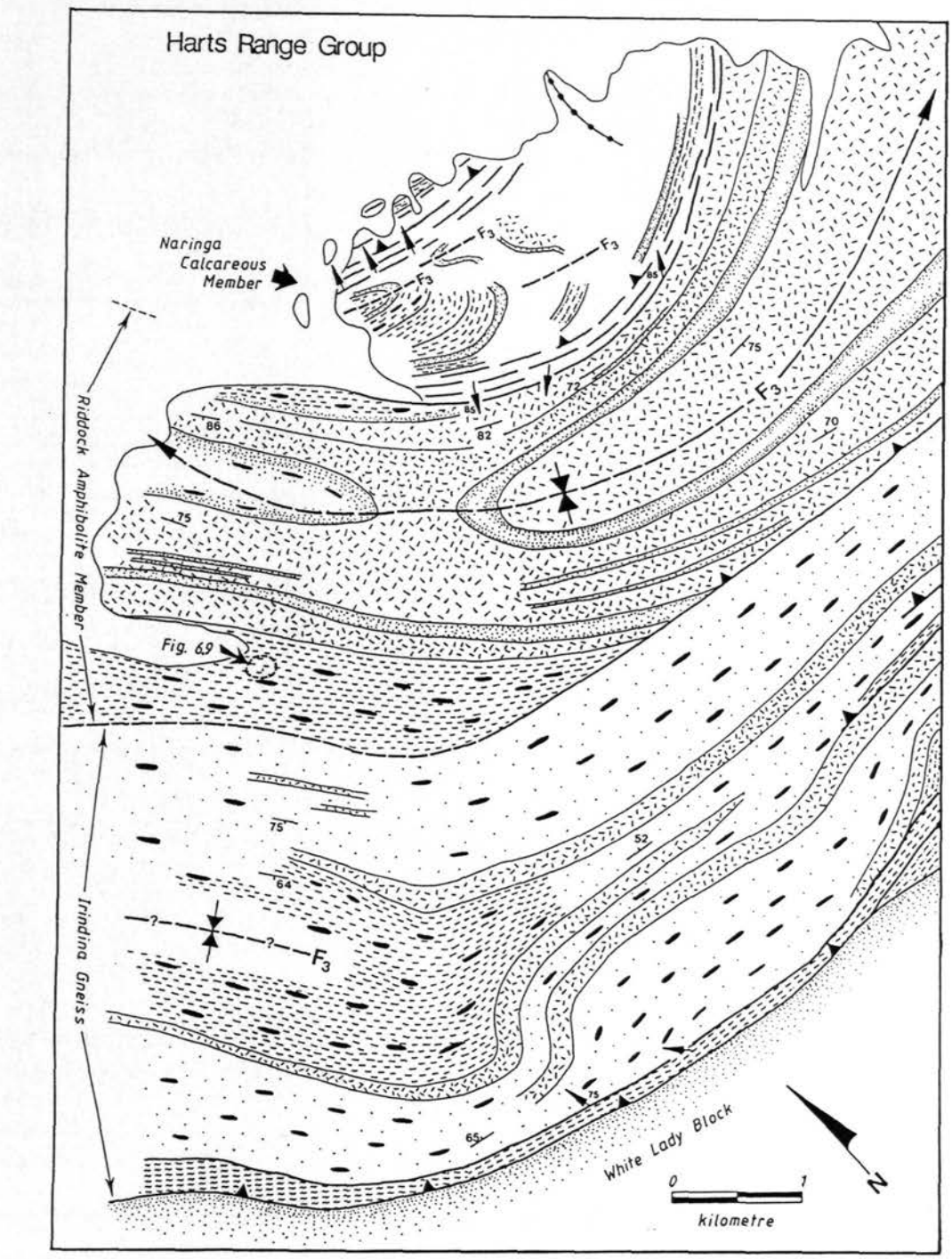

Cpx–Hbl–Pl±Qtz mafic gneiss

Cpx–Grt–Hbl–Pl±Qtz mafic gneiss

Grt–Pl–Qtz felsic gneiss and quartzite

interlayered felsic gneisses, quartzites, Sil–Grt–Bt gneisses and mafic gneisses

Sil–Grt–Bt–Kfs–Qtz gneiss

interlayered Sil–Grt–Bt felsic gneisses and mafic gneisses

calc–silicate rock

mylonite

67 mineral elongation azimuth and plunge

mylonitic foliation, reverse sense of sense of shear

78 strike and dip of S_2 foliation

Qtz–Kfs–Bt–Mu pegmatite

Fig. 6.6 Folded outcrop pattern of the Harts Range Group.

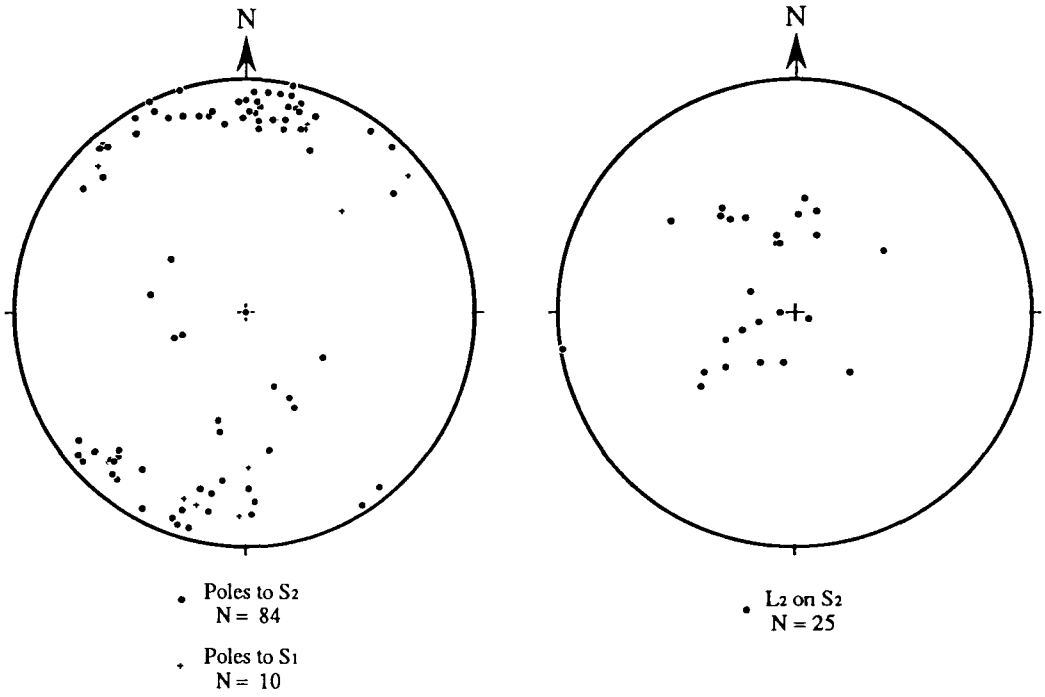

Fig. 6.7 Lower hemisphere, equal area, stereographic projections of poles to S_1 and S_2, and L_2 from the Riddock Amphibolite Member, Harts Range Group.

clinopyroxene-amphibole-plagioclase±garnet±quartz. S_2 is commonly sub-parallel to compositional boundaries but, due to the intensity of deformation associated with the development of S_2, the compositional layering has been rotated into parallelism with S_2. Any evidence for earlier deformations has been obliterated by recrystallization during peak metamorphism and D_2 deformation, which produced the pervasive S_2 foliation. The gross compositional boundaries are deformed and mafic layers are commonly boudinaged. No evidence for a primary sedimentary or igneous layering has been recognized and the gross compositional boundaries are referred to as S_1.

Anatexis accompanied peak metamorphism (M_1) and deformation and crystallization of leucosome in a tectonic foliation (S_2) during D_2. There appears to be no large-scale repetition of "stratigraphy" associated with D_1 nor D_2, and M_1 and S_2 mineral assemblages indicate that peak metamorphism was followed by cooling with limited decompression (Chapter 4). S_2 in the Harts Range Group is similar to S_2 in the Strangways Metamorphic Complex and was probably produced during a similar ductile non-coaxial deformation event (D_2). S_2 is oriented parallel to the axial plane of folded plagioclase leucosome, which defines F_2. Asymmetrical mafic boudins and folds are also common. Coarse-grained plagioclase-hornblende pegmatite networks commonly cut S_2, but contain an alignment of hornblende that is parallel to S_2. These pegmatite networks are inferred to have crystallized from partial melt during cooling from the metamorphic peak. They are correlated with similar late-D_2 pegmatite pods and networks in the Strangways Metamorphic Complex.

S_1 and S_2 are folded by east-west trending, upright, tight to isoclinal F_3 folds with shallow plunges that form the dominant macroscopic fold pattern of rock units in the Harts Range Group. Lineated hornblende occurs along the hinge of F_3 folds in the Riddock Amphibolite. The axial plane of the macroscopic F_3 fold in Fig. 6.6 dips steeply to the north and the fold axis is curved in the axial plane. The fold axis dips between 10-20° to the west and east. The axial plane is also curved, which is probably due to subsequent deformations. An early mineral elongation lineation is preserved on

the limbs of the large doubly plunging F_3 fold in Fig. 6.6 away from the fold hinge. This lineation is defined by elongate dimensions of plagioclase, clinopyroxene and hornblende and is referred to herein as L_2. L_2 is probably aligned parallel to the finite extension direction during D_2 and therefore is parallel to the axis of tectonic transport inferred for D_2. The orientation of the D_2 tectonic transport axis can be reconstructed by rotating S_1 and S_2 to a horizontal position over a shallowly plunging fold axis with and azimuth of 100°. The azimuth of the D_2 tectonic transport axis in northeast-southwest.

D_3 deformation was responsible for the dominant upright F_3 fold pattern. F_3 folds have wavelengths of up to 1 km and an amplitude of greater than 500 m. S_1 and S_2 were symmetrically shortened along a northnortheast-southsouthwest axis during D_3. The amount of shortening is difficult to estimate because of the lack of stratigraphy, but was probably up to 50%. The shortening axis is subparallel to the trend of the D_2 transport axis that is indicated by the orientation of L_2. The upright style of folding and an inferred northnortheast-southsouthwest shortening axis during D_3 are similar to deformation in the Reynolds Range, which has been referred to as DII by Dirks and Wilson (1990). Similar structural and metamorphic characteristics across large portions of the Arunta Block are discussed later in this Chapter.

6.32 Structural geology of the Irindina Gneiss

The Irindina Gneiss is compc sed of sillimanite-biotite-garnet-bearing quartzofeldspathic gneisses, mafic gneisses and minor calc-silicate rocks. It is separated from the Riddock Amphibolite Member to the north by a north-dipping mylonite zone that contains a well-developed steep lineation defined by elongate sillimanite. Asymmetrical K-feldspar augen in the mylonite indicate a reverse sense of movement. Structural data from the Irindina Gneiss are presented on stereographic projections in Fig. 6.8 and outcrop sketches of deformed Irindina Gneiss are shown in Fig. 6.9.

Mafic layers up to 50 m wide are common in the Irindina Gneiss and are similar in composition to the Riddock Amphibolite Member. These wide mafic layers contain a

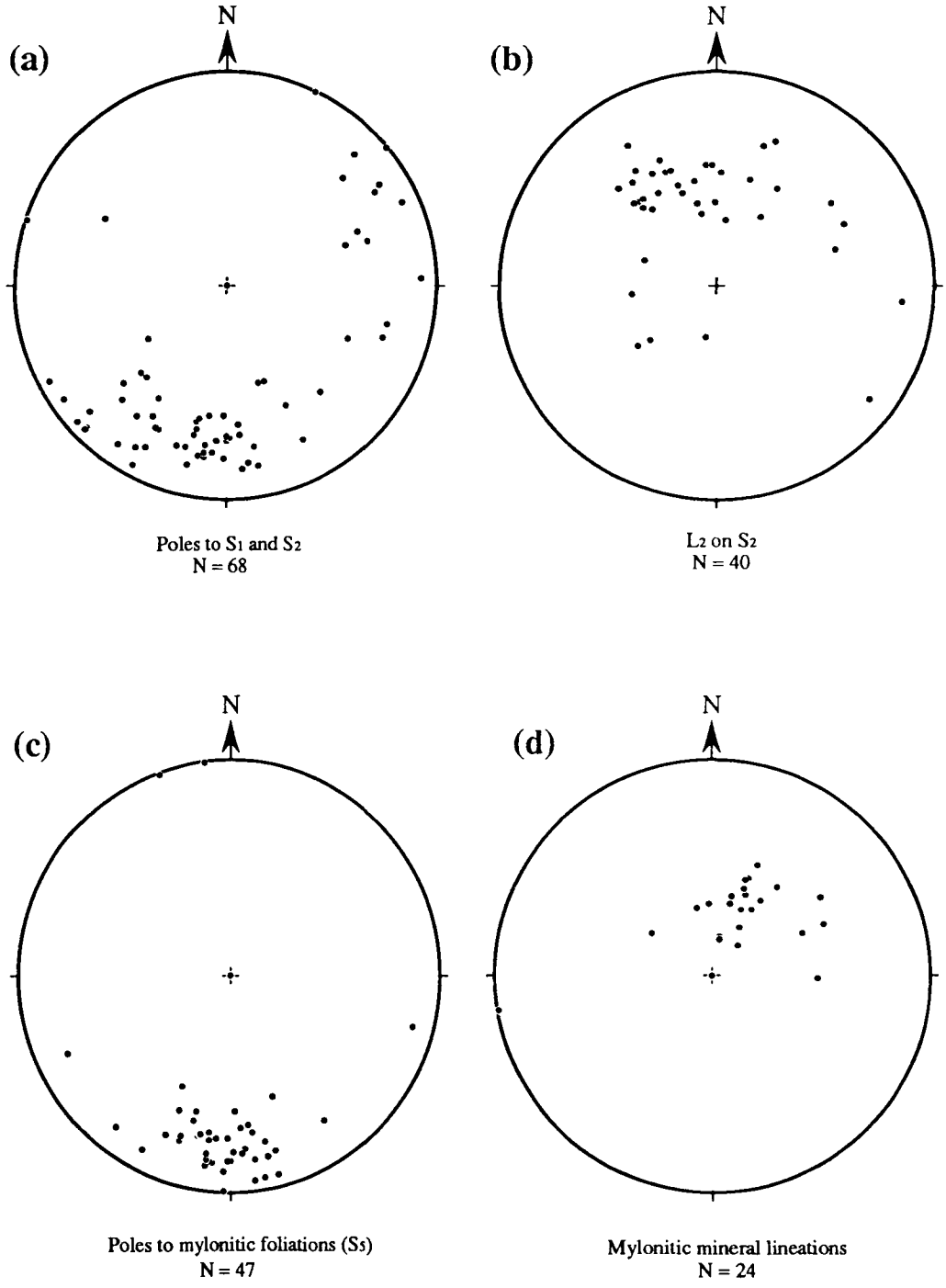

Fig. 6.8 Lower hemisphere, equal area, stereographic projections of structural data from the Irindina Gneiss.

6.8 (a) Poles to S_1 and S_2.

6.8 (b) Mineral elongation lineations (L_2) on S_1 and S_2.

6.8 (c) Poles to mylonitic foliations (S_5).

6.8 (d) Mineral elongation lineations (L_5) on S_5.

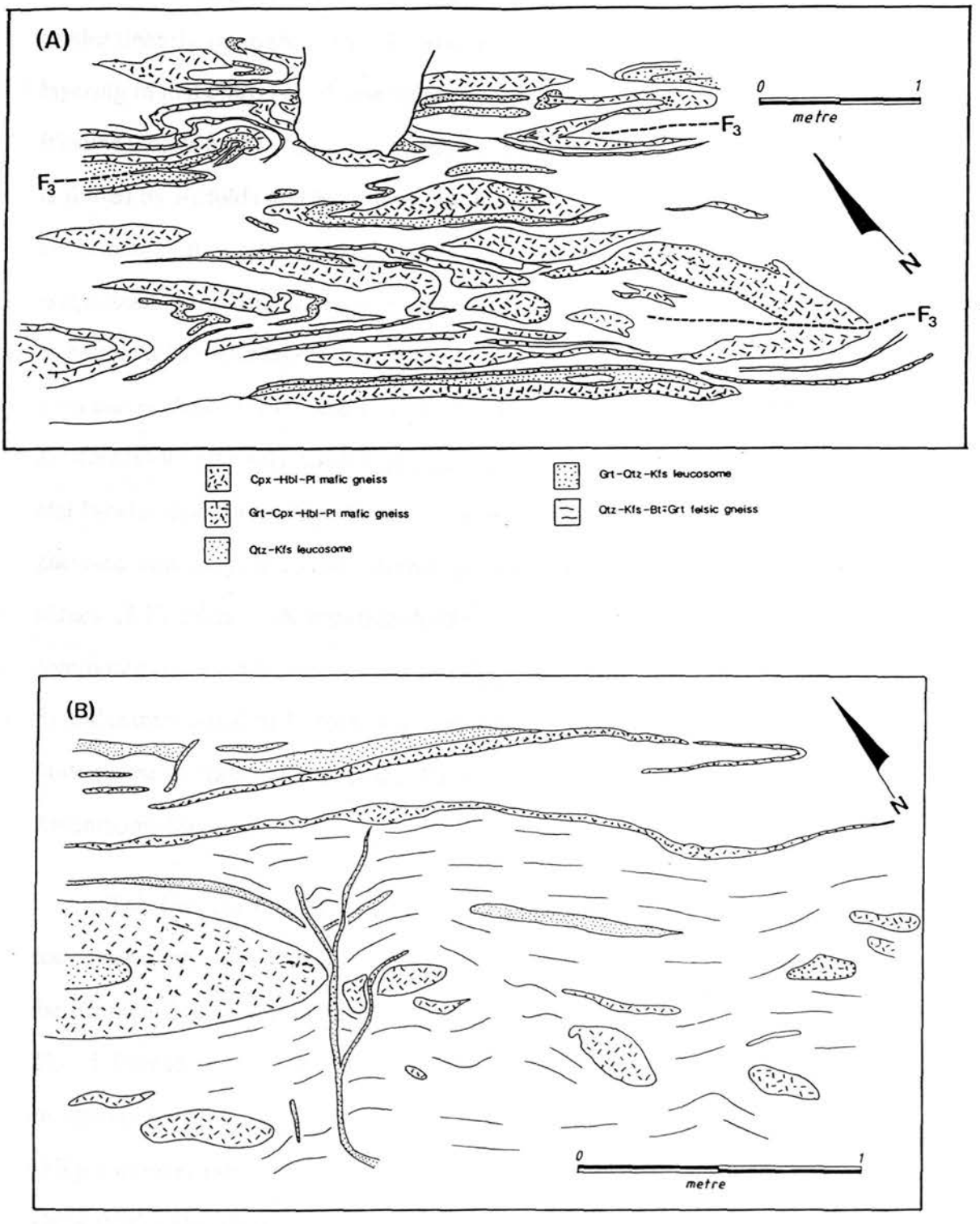

Fig. 6.9 Outcrop sketches of D_3 structures in the Irindina Gneiss. Locality is shown on Fig. 6.6.

cm-scale leucosome layering that resembles S_2 in the Riddock Amphibolite Member. Cm-scale coarse-grained pegmatite layers and garnet-bearing felsic leucosome in the predominantly quartzofeldspathic Irindina Gneiss are subparallel to the leucosome layering in mafic layers. These leucosome foliations are referred to as S_2. S_2 in the Irindina Gneiss has the same distribution as S_2 in the Riddock Amphibolite Member and is folded by F_3 folds that have steep north-dipping axial planes and shallow fold axes. Deformation of S_2 in the Irindina Gneiss is therefore correlated with D_3 in the Riddock Amphibolite Member. Garnet-bearing quartzofeldspathic pegmatite occurs in the necks of boudinaged mafic layers (Fig. 6.9b). The intensity of D_3 in the Irindina Gneiss was such that evidence for D_2 or any earlier deformations has been destroyed. Mafic layers are commonly intensely boudinaged and F_3 folds commonly have extremely attenuated and boudinaged limbs (Fig. 6.9a). Coarse-grained sillimanite and biotite in felsic gneisses, and recrystallized hornblende in mafic boudins are aligned parallel to the axial planes of F_3 folds. A lineation defined by elongate sillimanite, biotite and quartz commonly occurs in S_2 and plunges steeply to the north. This lineation is not folded by F_3 and is orthogonal to F_3 fold axes. It is referred to as L_3 and probably represents a finite extension direction during D_3. L_3 occurs along the same axis as L_2 in the Riddock Amphibolite Member.

The Irindina Gneiss crops out to the north of the White Lady Block, which comprises north-dipping, anastamosing shear zones. Adjacent to the White Lady Block, the Irindina Gneiss is also intensely deformed, in places, resembling an augen gneiss. This deformation is referred to as D_4. A quartz stretching lineation and sillimanite elongation lineation (L_4) is common and is subparallel to L_3. Asymmetrical augen and oblique mineral fabrics indicate that D_4 was characterized by non-coaxial deformation. These fabrics also preserve evidence for a reverse sense of movement.

D_4 mylonitic fabrics are deformed in northwest-verging steep crenulation zones (Fig. 6.6). These zones post-date folding and mylonitization of the Irindina Gneiss.

6.33 Structural geology of the Naringa Calcareous Member

The Naringa Calcareous Member crops out to the north of the Riddock Amphibolite Member. It is mostly composed of north-dipping augen gneiss, which preserves mineral fabrics that indicate intense non-coaxial deformation. However, less mylonitized folded gneisses also occur towards the centre of the outcrop. Structural data from the Naringa Calcareous Member are presented on stereographic projections in Fig. 6.10.

In this study area, the Naringa Calcareous Member comprises mainly quartzofeldspathic gneiss and minor biotite-sillimanite gneiss. Towards the centre of the outcrop a leucosome foliation is tightly folded about a steep northeast-plunging fold axis. The axial planes of these folds dip steeply to the north. These folds do not resemble folds in the Riddock Amphibolite Member nor the Irindina Gneiss, but resemble Type B F_3 mylonitic folds in the Strangways Metamorphic Complex. They are cut by a biotite foliation that forms a penetrative foliation in the augen gneisses. A quartz elongation lineation and an alignment of biotite in this foliation are parallel to the fold axes in the less deformed gneisses. Deformation on the Naringa Calcareous Member appears to be characterized by progressive non-coaxial deformation along a northeast-southwest axis, later deformation being concentrated into mylonite zones. Lineations in these mylonite zones and fold axes are parallel to L_3 lineations in the Irindina Gneiss and have the same azimuth as the shortening direction inferred for D_3 in the Riddock Amphibolite Member. Folding and mylonitization in the Naringa Calcareous Member is correlated with D_3 folding and D_4 mylonitization in the Riddock Amphibolite Member and Irindina Gneiss.

The reclined tight folds in the Naringa Calcareous Member are folded by open vertical folds, which have a north-south axial trace. These folds are probably related to east-west shortening after mylonitization. The mylonitic foliation is also deformed by crenulation zones. These zones have a steep north-plunging axis and commonly form

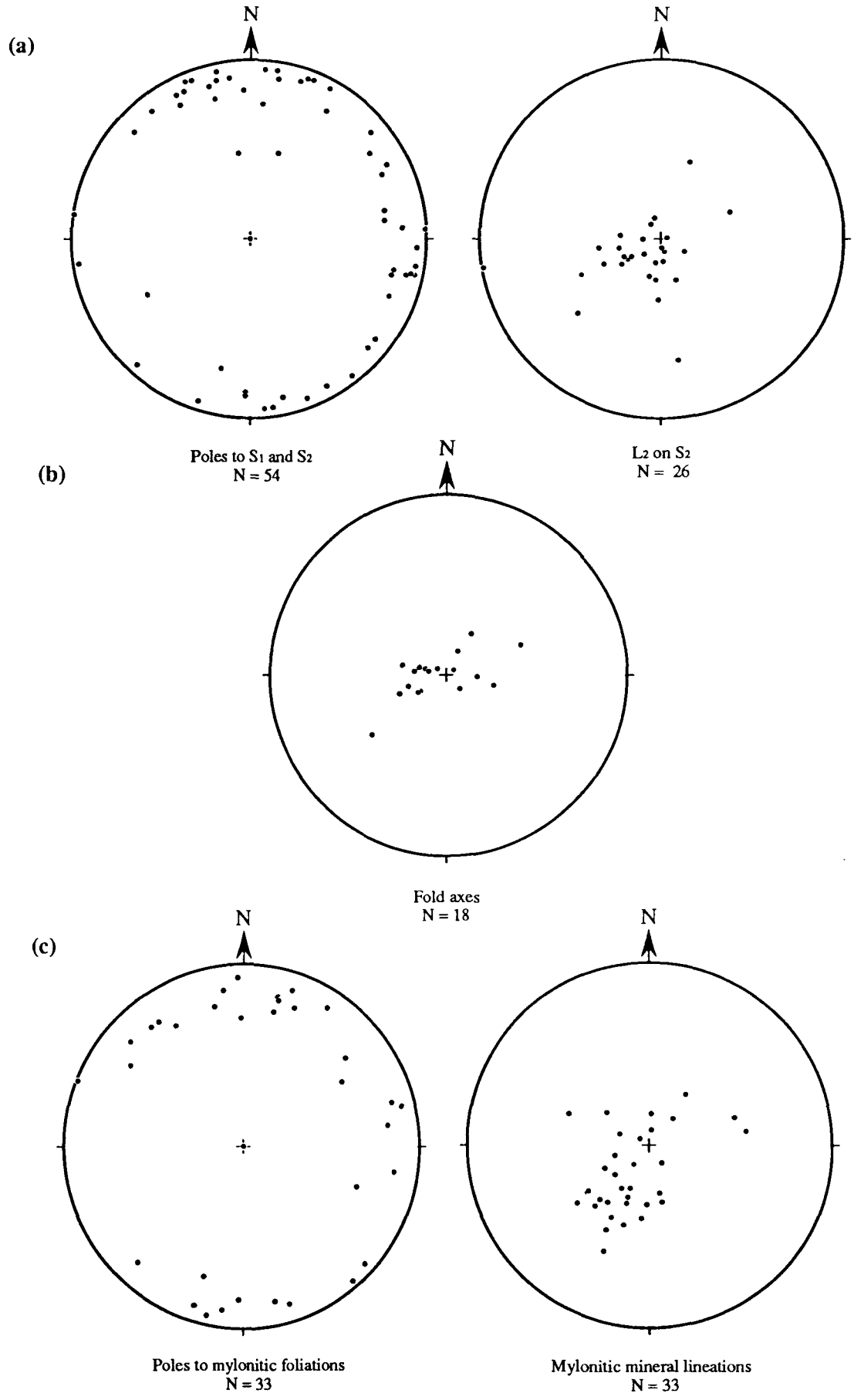

Fig. 6.10 Lower hemisphere, equal area, stereographic projections of structural data from the Naringa Calcareous Member, Harts Range Group.
6.10 (a) Poles to S_1 and S_2, and projections of L_2 on S_2
6.10 (b) F_3 fold axes
6.10 (c) Poles to mylonitic foliations and projections of mylonitic mineral lineations

conjugate sets that indicate north-south coaxial shortening. They may represent continual deformation after mylonitization during strain hardening as a result of cooling.

The upright open north-south folds and crenulation zones are cut by extensive pegmatite dykes that are commonly associated with greenschist facies retrogression.

6.34 Tectonometamorphic history of the Harts Range Group

Part of the tectonometamorphic evolution of the Harts Range Group can be attributed to two major deformation cycles, similar to those in the Strangways Metamorphic Complex. Deformation during the first deformation cycle (D_1-D_2) was accompanied by anatexis during peak metamorphism (M_1) and crystallization of leucosome in a tectonic foliation (S_2) during D_2. The orientation of S_2 is subparallel to the lithological layering and could have been initially recumbent. Mineral zoning indicates that peak metamorphism was followed by cooling and limited decompression (Chapter 4). D_2 structures in the Harts Range Group are similar to D_2 structures in the Strangways Metamorphic Complex and are indicative of extreme extension, which was probably associated with large simple shear strains. An L_2 lineation is preserved in the Riddock Amphibolite Member and indicates extension along a northeast-southwest axis. However, L_2 in the Strangways Metamorphic Complex has mostly been obliterated by intense recrystallization during D_3.

The similar orientation of structural fabric elements during D_3-D_4 suggests that they were produced during a continuous progressive deformational cycle. This deformation cycle was responsible for the upright fold pattern in the Riddock Amphibolite Member and Irindina Gneiss and reclined folds in the Naringa Calcareous Member (D_3), and mylonitization (D_4). The similar orientation of structural fabrics and inferred deformation axes in both the Harts Range Group and the Strangways Metamorphic Complex suggests that the D_3-D_4 deformation cycle in the Harts Range Group may have been contemporaneous with the Arunta Orogeny in the Strangways Metamorphic

Complex. The orientation of mineral fabrics in the mylonite zones indicates a probable northeast to southwest transport direction.

6.4 Shear zone deformation and metamorphic conditions

6.41 Deformation in the Gough Dam Schist Zone

The Gough Dam Schist Zone crops out on the northern margin of the Strangways Metamorphic Complex and consists of phyllonitic quartzofeldspathic gneisses, augen gneisses, biotite schists and residual pods of the Strangways Metamorphic Complex. (Fig. 1.0; Chapter 2). The Gough Dam Schist Zone contains a quartz rodding and a biotite±sillimanite elongation lineation that plunges to the northnortheast. Mineral fabrics indicate that deformation was characterized by both non-coaxial deformation and a flattening style of strain. Flattening strain postdated non-axial deformation and a southward sense of shear.

Lineations in the Gough Dam Schist Zone have a similar orientation to high-grade mineral lineations in a mylonitic foliation from the Erontonga metamorphics and the Anuma schist (sections 6.22 and 6.23). Deformation in the Gough Dam Schist Zone has been referred to as D_5 (Chapter 2) and postdated the dominant folding of both the Strangways Metamorphic Complex and the Harts Range Group. Staurolite-kyanite assemblages in the Anuma Schist are similar to assemblages that have been described from phyllonitic zones west of the Gough Dam Schist (Warren, 1983a). Coronas on kyanite described elsewhere appear to reflect isothermal uplift (Warren, 1983a) after deformation. Deformation in the Anuma schist and phyllonitic zones to the west probably correlate with D_5 deformation in the Gough Dam Schist Zone. The similar tectonometamorphic history in shear zones across the Arunta Block suggests that D_5 was a significant regional deformation a granulite facies conditions and predated isothermal uplift

Greenschist facies retrograde foliations postdate deformation associated with the formation of high-grade penetrative structural fabrics. Chlorite and muscovite-epidote

foliations commonly have a very oblique to subhorizontal east-west-trending mineral elongation. Greenschist facies retrogression was probably related to fluid movement and deformation during reactivation of the shear zones that separate the Strangways Metamorphic Complex and Harts Range Group.

6.42 Deformation in the White Lady Block

The White Lady Block (Shaw et al., 1984b) crops out to the north of the Gough Dam Schist Zone (Fig. 1.0). It comprises anastomosing, north-dipping ultramylonite zones and pods of mafic gneisses, quartzofeldspathic gneisses, sillimanite gneisses and minor megacrystic gneisses, similar to gneisses in the Strangways Metamorphic Complex. The outcrop pattern, which is shown in Fig. 6.11, resembles a tectonic mélange. Structural data from the White Lady Block are presented on stereographic projections in Fig. 6.12.

Ultramylonite zones in the White Lady Block preserve well-developed mineral fabrics indicate that deformation was non-coaxial and that south-directed shearing predominated. Evidence for mylonitic deformation also occurs in the Irindina Gneiss to the north. A gneissic tectonometamorphic foliation is preserved in the unmylonitized pods. This foliation has a similar distribution to S_2 in the Strangways Metamorphic complex and unlike the distribution of S_2 in the Harts Range Group (Fig. 6.12). These pods are probably reworked from the Strangways Metamorphic Complex. The mylonitic foliation contains a well-developed lineation defined by elongate quartz, feldspar and sillimanite, and aggregates of garnet and orthopyroxene. This lineation plunges consistently to the northnortheast (Fig. 6.12) and is subparallel to mineral elongation lineations in the Gough Dam Schist Zone. Metamorphic conditions during ultramylonitization in the White Lady Block were probably similar to conditions during D_4 ultramylonitization in the Strangways Metamorphic Complex on the basis of similarity in recrystallized mineral assemblages.

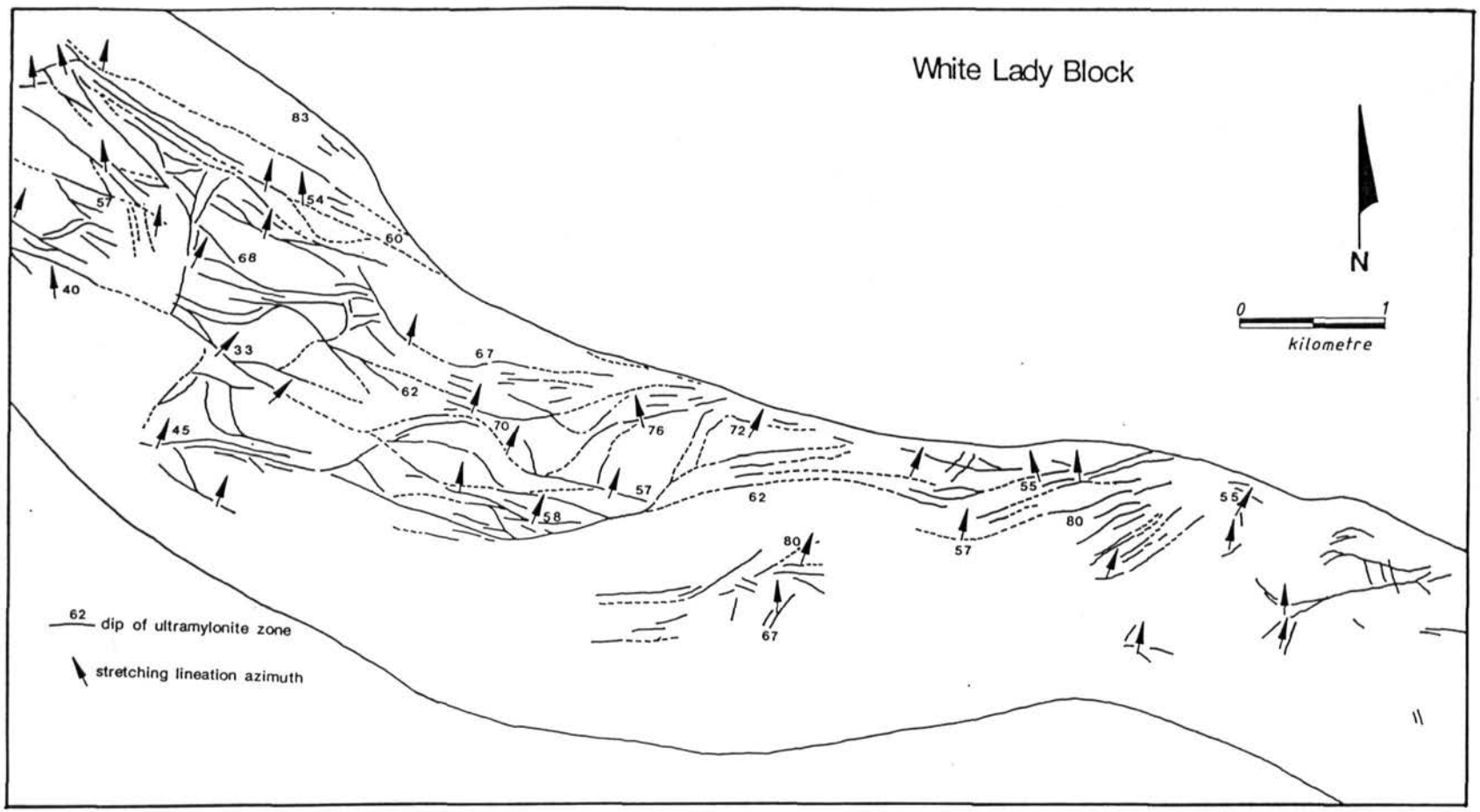

Fig. 6.11 Outcrop shear zone pattern in the White Lady Block.

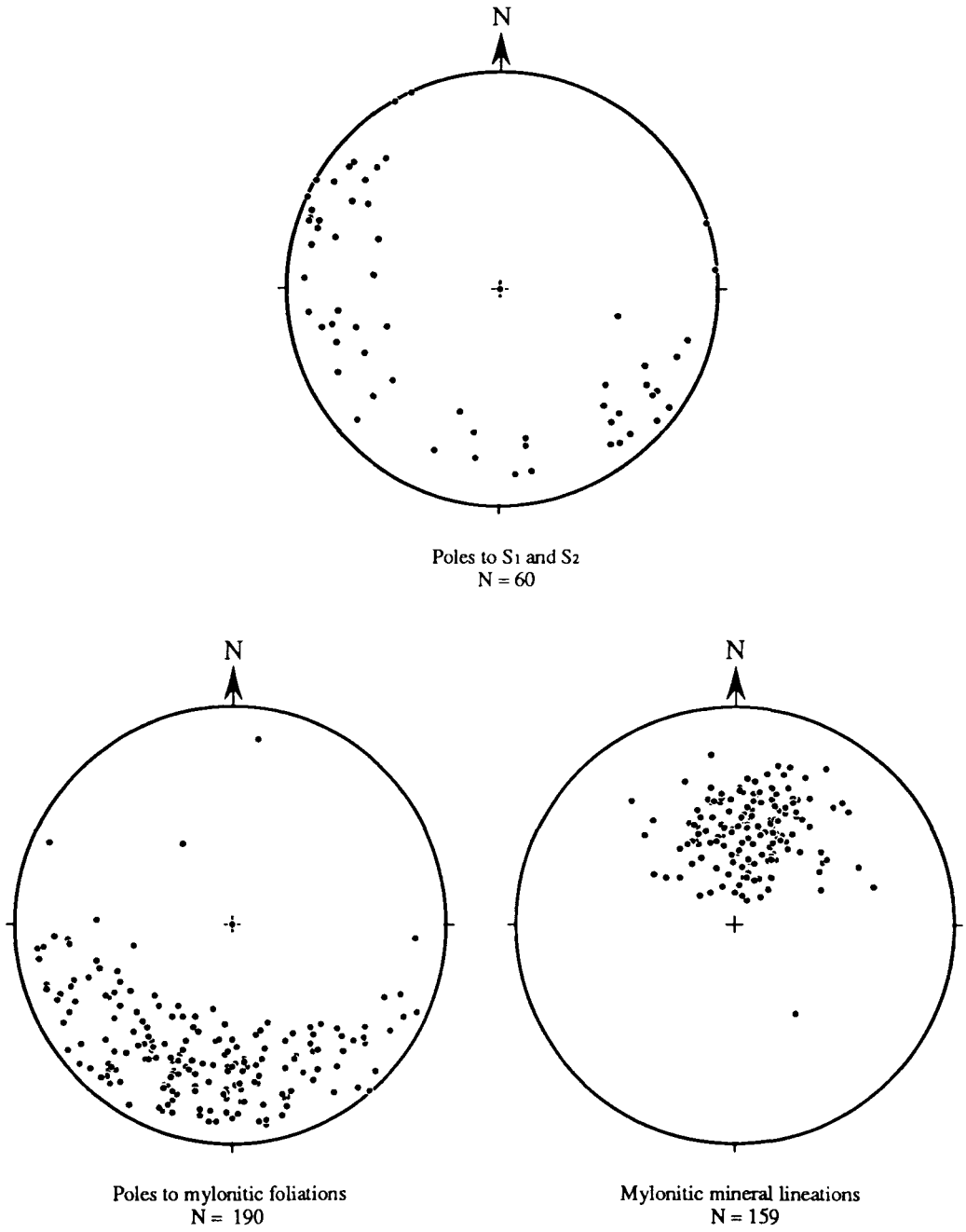

Fig. 6.12 Lower hemisphere, equal area, stereographic projection of poles to S_1 and S_2, and poles to mylonitic foliations and mylonitic lineations from the White Lady Block.

Deformation in the White Lady Block may have been responsible for juxtaposing the Harts Range Group (Fig. 1.0) against the Strangways Metamorphic Complex. James and Ding (1988) have suggested that a major crustal detachment between the Harts Range Group and the Strangways Metamorphic Complex was active when the Bruna Gneiss was intruded at 1747 Ma (Mortimer et al., 1987), thereby dating this thrusting event. On the basis of structural and metamorphic data from the Strangways Metamorphic Complex and Harts Range Group, it is also possible that non-coaxial deformation in high strain zones in the Gough Dam Schist Zone and the White Lady Block represents the continuation of a major progressive orogenic cycle.

6.43 The relationship between deformation in the Amadeus Basin and the central Arunta Block

Collins and Teyssier (1989) have interpreted deformation in the Bruna Gneiss and other shear zones between the Harts Range and the Amadeus Basin, to the south, to be have been part of a crustal-scale Palaeozoic deformation that produced the Arltunga Nappe Complex during the Alice Springs Orogeny in the mid-Carboniferous (Stewart, 1971). Palaeozoic deformation produced thrust sheets involving late-Proterozoic sedimentary rocks south of the Erontonga metamorphics, and a new tectonic fabric in the basement. Greenschist facies mineral fabrics in the Erontonga metamorphics and Anuma schist that were produced during the Alice Springs Orogeny are structurally distinct from the earlier deformation fabrics. On the basis of similar orientations of structural fabrics and similar successive mineral assemblages, high-grade deformation in the Erontonga metamorphics and the Anuma schist may correlate with D_5 deformation elsewhere in the Strangways Metamorphic Complex and D_4 in the Harts Range Group. Therefore, D_5 deformation in the Strangways Metamorphic Complex and D_4 in the Harts Range Group occurred prior to the Alice Springs Orogeny. However, D_5 and D_4 shear zones were probable conduits for fluid during retrogression and were partially reworked during uplift of the Arunta Block and deformation during the Alice Springs Orogeny.

6.5 Deposition of the Reynolds Range Group

During the early to mid-Proterozoic at least two episodes of sedimentation alternated with large scale orogenic events in the Arunta Block (Stewart et al., 1984; Shaw et al., 1984a). Shallow-marine siliciclastic and carbonate deposits belonging to the 1800 Ma old Reynolds Range Group represent a transgressive sequence deposited during the last depositional episode on a low-gradient shelf, that was affected by long-shore currents, tidal currents, storm wave action, and fair-weather wave action (Dirks and Norman, 1991; Appendix). An angular unconformity separates the Reynolds Range Group from the underlying Lander Rock Beds (Stewart et al., 1980). The Reynolds Range Group consists of a 1100 m thick sequence comprising basal conglomerate and massive quartzite, mudstone and calcareous rocks. The concentration of southwest-directed palaeocurrent directions and facies distribution (Dirks, 1991) suggests that a low-gradient palaeo-shelf extended towards the southwest. Vertical and lateral stratigraphic transitions between the facies associations are generally gradational, which may reflect coeval coexistence of all facies on the shelf and small, net, relative sea level changes. Long-shore currents were subordinate on the middle shelf, but were dominant on the inner shelf, where they influenced the southeastward migration of large sand wave complexes. Storms were mainly erosional on the inner shelf and carried large volumes of clastic sediment to the middle shelf, where it was deposited in extensive quartz-sandstone sheets. The non-barred nature of the coastline, as well as a lack of tidal inlet and delta deposits, suggests a low tidal range. Where the input of siliciclastic sediment was low, build-ups of shallow-water carbonate deposition, associated with stromatolites, formed on the middle shelf (Dirks and Norman, 1991; Appendix).

The Lander Rock Beds, which unconformably underlie the Reynolds Range Group, are complexly deformed and metamorphosed. Peak metamorphism was diachronous with the development of a layer-parallel foliation (Vernon et al., 1990) and probably occurred at about 1820 Ma (Clarke et al., 1990). The Reynolds Range Group is intruded by the Napperby Gneiss. An emplacement age of 1760 Ma is interpreted

from zircon ages in the Napperby Gneiss (Collins et al., 1991). The age of peak metamorphism in the Lander Rock Beds and the intrusion of the Napperby Gneiss constrains deposition of the Reynolds Range Group to be between 1820 Ma and 1760 Ma. Deposition of the Reynolds Range Group coincides with interpreted ages of cooling during D_2 in the Strangways Metamorphic Complex (Chapter 2). The possible relationship between deformation and metamorphism in the Strangways Metamorphic Complex and deposition in the Reynolds Range Group and Hatches Creek Group is discussed in the next section. The Reynolds Range Group also probably correlates with sediments and volcanics belonging to the Hatches Creek Group in the Davenport Province, north of the Arunta Block (Shaw and Stewart, 1975; Blake, 1984). The Hatches Creek Group is a transgressive sequence and was probably initiated by rift-related faulting, as evidenced by bimodal volcanics occurring at the base of the Group and (Blake et al., 1986). These sediments were deposited between 1820 Ma and 1800 Ma (Blake and Page, 1988) and display similar upright folds (Blake et al., 1986) to the Reynolds Range Group and the Harts Range Group.

U/Pb isotopic studies of zircons suggest that another granulite facies metamorphism occurred at about 1730 Ma (Collins et al., 1991), which affected the Reynolds Range Group. This metamorphism was probably concomitant with the southeast-trending, upright folding that produced the dominant macroscopic fold pattern in the Reynolds Range (Dirks and Wilson, 1990).

Extensive deposits of inner-shelf sand, development of barrier island coasts and the shape of the shelf can be related to tectonic processes. Modern coasts can be divided into collisional, trailing edge and marginal seas (Inman and Nordstrom, 1971). A shallow, wide, low-gradient, marine shelf that existed during deposition of the Reynolds Range Group is typical of a trailing edge (Afro-type) coast or epeiric sea coast. Precambrian supracrustal deposits such as the Reynolds Range Group are important because they may reflect crustal responses to lithosphere and mantle processes that were restricted to the Precambrian (Plumb, 1979; Etheridge et al., 1987; Condie, 1982).

Shortening along a northeast-southwest axis during the upright folding of the Reynolds Range Group was parallel to the shelf gradient and perpendicular to the palaeo-shoreline. Rapid uplift, erosion, basin formation, deposition and closure of the Reynolds Range Group may have been part of related tectonometamorphic processes.

6.6 Regional correlations

In order to delineate the tectonic processes that may have responsible for deformation and metamorphism in the Arunta Block, it is necessary to correlate regional tectonic events, where possible, and to recognize parallels in the tectonometamorphic evolution of different terrains. For example, deposition of the Reynolds Range Group was probably concurrent with deposition of the Hatches Creek Group in the Davenport Province and may have been concomitant with cooling during D_2 in the Strangways Metamorphic Complex. The earliest metamorphisms in the northern Arunta Block are characterized by typical Proterozoic high-temperature, low-pressure conditions and occurred within a similar time span as M_1/D_1 and D_2 in the Strangways Metamorphic Complex, namely 1820-1760 Ma (Vernon et al., 1990; Clarke et al., 1990; Dirks and Wilson, 1990). Although high-grade peak metamorphisms in the northern Arunta Block are temporally distinct, they have been inferred to reflect successive local thermal perturbations (Clarke et al., 1990). The cause of these metamorphic events probably involved advection (Vernon et al., 1990) and the contact effects of large granitoid intrusions. A similar heat source that was external to the crust and mantle lithosphere could also be inferred for M_1 metamorphism and D_1-D_2 deformation in the central Arunta Block.

Age constraints for deformation and metamorphism in the northern Arunta Block (Clarke et al., 1990) suggest that intrusion of the Napperby Gneiss into the Lander Rock Beds occurred at the same time as peak metamorphism in the Strangways Metamorphic Complex. Metamorphism and deformation in the Lander Rock Beds occurred before intrusion of the Napperby Gneiss. The Lander Rock Beds could be equivalent to the Strangways Metamorphic Complex or older. They certainly cannot be younger or part of

the stratigraphically higher Division 2 sequence, as suggested by Stewart et al. (1984). Similarly, if the Harts Range Group and the Strangways Metamorphic Complex were part of the same protolith (Chapter 4), the Harts Range Group also cannot belong to the Division 2 rocks of Stewart et al. (1984). Although rocks belonging to the Reynolds Range Group form a younger unconformable sequence, the use of the Division concept for older rock units such as the Strangways Metamorphic Complex, Lander Rock Beds and the Harts Range Group appears to be invalid.

Deformation and metamorphism of the Reynolds Range Group, referred to as DII, MII by Dirks and Wilson (1990), occurred at about 1730 Ma (Clarke et al., 1990). This deformation produced large south-east trending upright folds (Dirks and Wilson, 1990), similar to the dominant, macroscopic folds in the Harts Range Group. Upright folding and concomitant metamorphism in the Reynolds Range and Harts Range may correlate with a major compressional tectonometamorphic event in the Strangways Metamorphic Complex, which produced large-scale mylonitic folds and is thought to have occurred at about 1745 Ma (Chapters 2 and 3). High-grade extensive shear zones with a southward tectonic transport were probably produced during the later part of the deformation. This tectonometamorphic event was distinct from earlier deformations and metamorphisms, which have been attributed to thermal perturbations external to the crust.

In the southern Arunta Block, Division 3 metasediments comprising the Chewings Range Quartzite probably correlate with sediments belonging to the Reynolds Range Group (Shaw and Wells, 1983). However, the structural evolution of the Chewings Range Quartzite (Teyssier et al., 1988) differs from that of the Reynolds Range Group (Dirks and Wilson, 1990). The earliest deformations in the Chewings Range Quartzite are characterized by a complex horizontal deformation with a northward tectonic transport (Teyssier et al., 1988). Later deformations produced east-west south-verging horizontal folds and ductile faults that preserve a south-directed sense of movement and are similar to structures in the northern and central Arunta Block.

6.7 Models of early- to mid-Proterozoic tectonism in the Arunta Block

Similar structural and metamorphic histories of mid-crustal rocks from the central and northern Arunta Block and the depositional, structural and metamorphic history of Division 3 sediments in the Arunta Block place constraints on the interpretation of Proterozoic tectonic environments. Two tectonometamorphic cycles are recognized in rocks from the Strangways Metamorphic Complex and northern Arunta Block and are inferred to reflect two distinct and different tectonic settings. Whereas the metamorphic and structural evolution of Phanerozoic orogens can be well constrained and related to plate tectonic processes, extrapolation of modern tectonic processes to explain the metamorphic and structural evolution of high-grade Proterozoic gneissic rocks is either difficult or impossible.

Tectonic models that may explain the high geothermal gradient recorded by granoblastic mineral assemblages in gneisses from the central Arunta Block have been alluded to in previous sections. Asthenospheric thermal perturbations may have been related to locally increased geothermal gradients (Clarke et al., 1990). However, it seems unlikely that advection involving granites and a significant underplate would raise the mid-crustal geotherm in the Strangways Metamorphic Complex to as much as 55°C/km, according to Bohlen (1991) and Loosveld and Etheridge (1990). Continental and lithospheric extension are also known to increase the geothermal gradient (Wickham and Oxburgh, 1985; Lachenbruch, 1979) and lithospheric extension has been proposed as a mechanism to produce high-temperature, low-pressure metamorphism in the base of the crust (Sandiford and Powell, 1986). The model of McKenzie (1978) for lithospheric extension involved uniform stretching or pure shear. Other extensional models accommodate slip along low-angle detachment systems that may penetrate the whole lithosphere and involve bulk simple shear extension (Wernicke, 1985) or low-angle crustal detachments and pure shear extension of the mantle lithosphere (Lister and Davis, 1983).

On the basis of the preceding arguments a high heat flow at mid-crustal levels could be explained by a model of lithospheric extension augmented by magmatic accretion and advection. Such processes may have been involved in the earliest tectonometamorphic cycle in the Arunta Block. Platform sediments in the Reynolds Range Group and extensive platform sediments and bimodal volcanics in the Davenport Province, north of the Arunta Block, may have been deposited during thermal relaxation in a deepening intracratonic basin that coincided with maximum crustal extension. Thermal decay and relaxation would occur after the metamorphic peak. Interpreted age constraints for deposition of the Reynolds Range Group and M_1 and D_2 in the Strangways Metamorphic Complex suggest that deposition occurred after M_1. Maximum crustal extension would be asymmetrical to maximum lithospheric thinning and therefore the greatest geothermal gradient. The variation in peak metamorphic grade across the terrain and the geometry of the shelf or basin in which sediments were deposited during thermal relaxation would be determined by the geometry of the detachment system. Correlation of the Hatches Creek Group and the Reynolds Range Group suggests that maximum crustal extension occurred to the north and that a continental shelf dipped to the southwest. The geometry of early-mid Proterozoic deposition could be explained by a southwest-dipping detachment system (P. H. Dirks, pers comm., 1990). A southward increase in the metamorphic gradient during M_1 in mid-crustal rocks from the central Arunta Block (Chapter 4) also suggests that extension was asymmetrical and involved a south-dipping detachment system.

Initial isobaric cooling following peak metamorphism can result from collisional (Ellis 1987) or extensional (Sandiford and Powell, 1986) tectonics. However, the inferred P-T-t paths are different. Although evidence for the early tectonometamorphic history of the central Arunta Block has been obliterated during prograde metamorphism, S_1 sillimanite inclusion trails and the lack of high-pressure mineral inclusions suggest that the prograde P-T-t path occurred in the sillimanite stability field and probably involved an anticlockwise path rather than a clockwise path with pressure increasing with temperature. Cooling after peak metamorphism in the central Arunta Block was

accompanied by limited decompression (Chapter 4). Due to the lack of structures indicative of crustal shortening during prograde metamorphism, magmatic thickening of the crust is assumed to have accompanied lithospheric thinning in the central Arunta Block (Chapter 2). Granitic gneisses, such as the Napperby gneiss in the northern Arunta Block, rose through the crust and spread out horizontally near the surface (in low-pressure terrains) as gravitational equilibrium was approached. Crustal thickening by overaccretion could have been augmented by significant underplating. Therefore, a tectonic model for the early evolution of the Arunta Block probably involved lithospheric thinning and crustal thickening due to magmatic accretion.

Following the culmination in magmatism and metamorphism, the crust began to cool (Chapters 2 and 4). In order to maintain isostatic equilibrium, limited uplift occurred during cooling. This may have triggered a gravitational instability and partial collapse of the crust, which resulted in non-coaxial, ductile, layer-parallel extension (c.f. Sandiford, 1989a). A northeast-southwest tectonic transport axis during extension is preserved as a mineral elongation lineation (L_2) in the Harts Range Group. This is perpendicular to the inferred trend of a extensional detachment during peak metamorphism. Cooling may well have been accompanied by the formation of eclogite in the lowermost crust (Bohlen, 1991). Continual cooling of the terrain and thermal relaxation allowed the Hatches Creek depositional basin to extend towards the southwest. The geometry of an inferred extensional system is important in determining the shape of a subsiding basin, amount of uplift of the surrounding highlands, erosion rates and the life of the sedimentary basin (Morley 1989). A steep boundary fault (60°-70°) with a large depth (30 km) to detachment can result in a thick sedimentary sequence and large vertical displacement compared to horizontal displacement. With only small amounts of horizontal displacement, the rotation of the hanging wall would produce large strains that become inefficient at depth. Consequently, the high-angle boundary fault must evolve into a shallow detachment or cease to be active (Morley, 1989). Another consequence of large rotational strains could be to initiate crustal instabilities in the hanging wall that result in the horizontal collapse or shortening of the sedimentary basin towards the

footwall. Following deposition of the Reynolds Range Group, the northern and central Arunta Blocks were deformed during northeast-southwest crustal shortening, perpendicular to the mid-Proterozoic shoreline.

The second tectonometamorphic cycle was unlike the first, because the preserved structures and metamorphic assemblages imply significant horizontal shortening and tectonic thickening of the crust. However, there are no obducted ophiolite remnants nor blueschist facies assemblages that are products of accretion and collision at convergent plate margins. There is also no evidence for isothermal decompression after M_2 in rocks from the Strangways Metamorphic Complex, which would be expected as an isostatic response to tectonic thickening. Although an increase in temperature and pressure associated with deformation are characteristic of compressional tectonics, the second tectonometamorphic cycle is unlike a normal Wilson cycle, which preserves a clockwise P-T-t path. An interpretation of the tectonic setting for the second metamorphic cycle is further complicated because the inferred tectonic transport directions in the southern Arunta Block (Teyssier et al., 1988) are opposite to those in the northern and central Arunta Blocks. The lack of an isostatic response to an increase in pressure during M_2 in the Strangways Metamorphic Complex suggests that either tectonic thickening during shortening was not great or that crustal thickening itself was a means of maintaining isostatic equilibrium. Loosveld and Etheridge (1990) have suggested that crustal thickening may occur during convective thinning of the mantle lithosphere. In their model isobaric cooling follows metamorphism and there is no significant isostatic uplift. The tectonic setting for the second tectonometamorphic event could have also involved thinning of the mantle lithosphere. Cooling from peak metamorphism may have converted the basal crust to eclogite (Bohlen, 1991) and delamination of the crust (Bird, 1979; Bird and Baumgardner, 1981) may have occurred when the dense eclogite sank into the asthenosphere, which has been called A-subduction by Kröner (1985). However, the inferred short period of time between peak metamorphism and the second tectonometamorphic event (70-50 Ma) may not have been sufficient to form eclogite at the base of the crust. Rather than initiating uplift, as suggested by Bohlen (1991),

crustal delamination could have resulted in significant crustal gravitational instabilities (e.g. Sandiford, 1989a) and may have caused an inward collapse of the crust. Alternatively, shortening of the crust could have been intracratonic deformation related to the tectonic evolution of a plate margin elsewhere.

The style of deformation in the Strangways Metamorphic Complex differed from that in the Harts Range Group. Non-coaxial deformation dominated in the Strangways Metamorphic Complex and produced mylonitic folds. Deformation was probably enhanced by an increased fluid activity, which caused strain softening (Chapter 1). However, deformation in the Harts Range Group produced predominantly upright isoclinal folds. A lower temperature and fluid activity in the Harts Range Group (Chapter 4) during the second tectonometamorphic cycle probably resulted in structures more typical of coaxial strain in rigid blocks between non-coaxial shear zones. Progressive deformation during this tectonometamorphic cycle resulted in deformation being concentrated into localized zones of non-coaxial strain, and migration of the deformation front southwards towards the southern Arunta Block (D_3-D_4 deformation of Teyssier et al., 1988).

6.7 Conclusions

The arrangement of kinematic fabrics and successive mineral assemblages in the Strangways Metamorphic Complex and Harts Range Group indicate that the central Arunta Block underwent two major tectonometamorphic events in the early- to mid-Proterozoic. The main features of the tectonic evolution that were interpreted from detailed study of the structural and metamorphic fabrics are:

(1) Peak metamorphism occurred at high temperatures and low to intermediate pressures.

(2) The inferred peak metamorphic geotherm increased southwards.

(3) Similar inferred P-T-t paths and tectonometamorphic fabrics suggest that the Harts Range Group and the Strangways Metamorphic Complex may have been part of the same protolith.

(4) A layer-parallel tectonic foliation developed during and after peak metamorphism and was probably due to intense non-coaxial ductile extension along a northeast-southwest axis at about 1765 Ma.

(5) Limited decompression occurred during cooling and was accompanied by the crystallization of partial melts.

(6) Intrusion of the Anamarra Granite occurred about 20 Ma after D_2 and 55 Ma after M_1.

(7) A major deformational cycle affected the Strangways Metamorphic Complex after the metamorphic peak and was accompanied by an increase in temperature and pressure.

(8) Mylonitic folding in the Strangways Metamorphic Complex is correlated with upright folding in the Harts Range Group.

(9) The second deformational cycle was progressive and resulted in sillimanite- and staurolite-bearing shear zones that traverse the entire central Arunta Block.

(10) Isothermal uplift did not occur immediately after the second tectonometamorphic event.

On the basis of regional correlations, the two tectonothermal events recognized in the central Arunta Block appear to have affected large portions of the Arunta Block. The early- to mid-Proterozoic tectonic evolution of the Arunta Block is inferred to have involved: (1) asymmetrical lithospheric extension and concomitant crustal thickening due to magmatic accretion; (2) thermal relaxation, ductile extension and deposition of supracrustal rocks; (3) possible conversion of the base of the crust to eclogite and crust/mantle delamination; (4) crustal shortening and thickening; (5) isobaric cooling at depth until uplift and erosion during deposition of the Heavitree Quartzite in the late-Proterozoic.

REFERENCES

Aigner, T. and Reineck, H. E., 1982. Proximality trends in modern storm sands from the Helgoland Bight (North Sea) and their implications for basin analysis. *Senckenbergiana Maritima*, **14**, 183-215.

Allen, A. R., 1979. Metasomatism of a depleted granulite facies terrain in the Arunta Block, central Australia. 1. Geochemical evidence. *Contributions to Mineralogy and Petrology*, **79**, 319-332.

Allen, A. R. and Stubbs, D., 1982. An 40Ar/ 39Ar study of a polymetamorphic complex in the Arunta Block, central Australia. *Contributions to Mineralogy and Petrology*, **79**, 319-332.

Allen, J. R. L., 1982. *Sedimentary structures: their character and physical basis*; volume 1. Elsevier, Amsterdam, 593 pp.

Austrheim, H. and Griffin, W. L., 1985. Shear deformation and eclogite formation within granulite-facies anorthosites of the Bergen Arcs, Western Norway. *Chemical Geology*, **50**, 267-281.

Behrmann, J. H. and Mainprice, D., 1987. Deformation mechanisms in a high-temperature quartz-feldspar mylonite: evidence for superplastic flow in the lower continental crust. *Tectonophysics*, **140**, 297-305.

Bell, T. H., 1978. Progressive deformation and reorientation of fold axes in a ductile mylonite zone: The Woodroffe Thrust. *Tectonophysics*, **44**, 285-320.

Bell, T. H. and Etheridge, M. A., 1973. Microstructures of mylonites and their descriptive terminology. *Lithos*, **6**, 337-348.

Bell, T. H. and Hammond, 1984. On the internal geometry of mylonite zones. *Journal of Geology*, **92**, 667-686.

Berthé, D., Choukroune, P. and Jegouzo, P., 1979. Orthogneiss, mylonite and non-coaxial deformation of granites: and example of the South Armorican Shear-zone. *Journal of Structural Geology*, **1**, 31-42.

Bertrand-Sarfati, J. and Moussine-Pouchkine, A., 1988. Is cratonic sedimentation consistent with available models? An example from the Upper Proterozoic of the West African Craton. *Sedimentary Geology*, **58**, 255-276.

Bhatia, M. R. and Taylor, S.R., 1981. Trace-element geochemistry and sedimentary provinces: a study from the Tasman geosyncline, Australia. *Chemical Geology*, **33**, 115-125.

Bird, P., 1979. Continental delamination and the Colarado Plateau. *Journal of Geophysical Research*, **84**, 7561-7571.

Bird, P. and Baumgardner, J., 1981. Steady propagation of delamination events. *Journal of Geophysical Research*, **86**, 4891-4903.

Black, L. P., Shaw, R. D. and Offe, L. A., 1980. The age of the Stewart Dyke swarm and its bearing on the onset of later Precambrian sedimentations in central Australia. *Journal of the Geological Society of Australia*, **27**, 151-155.

Black, L. P., Shaw, R. D. and Stewart, A. J., 1983. Rb-Sr geochronology of Proterozoic events in the Arunta Inlier, central Australia. *Bureau Mineral Resources, Geology and Geophysics, Journal*, **8**, 129-138.

Blake, D. H., 1984. Stratigraphic correlations in the Tennant Creek Region, central Australia: Warramunga Group, Tomkinson Creek beds, Hatches Creek Group and Rising Sun Conglomerate. *Bureau of Mineral Resources, Journal of Australian Geology and Geophysics*, **9**, 44-47.

Blake, D. H. and Page, R. W., 1988. The Proterozoic Davenport Province, central Australia: regional geology and geochronology. *Precambrian Research*, **40/41**, 329-340.

Blake, D. H., Stewart, A. J.and Sweet, I. P., 1986. The Proterozoic Hatches Creek Group, an ensialic sandstone-bimodal volcanic association in central Australia. *Transactions of the Geological Society of South Africa*, **89**, 243-251.

Boettcher, J., 1970. The system CaO-Al_2O_3-SiO_2-H_2O at high pressures and temperatures. *Journal of Petrology*, **11**, 337-379.

Bohlen, S. R., 1987. Pressure-temperature-time paths and a tectonic model for the evolution of granulites. *Geology*, **95**, 617-632.

Bohlen, S. R., 1991. On the formation of granulites. *Journal of Metamorphic Geology*, **9**, 223-229.

Bohlen, S. R., Wall, V. J. and Boettcher, A. L., 1983. Geobarometry in granulites. In: *Kinetics and equilibrium in mineral reactions* (edited by Saxena, S. K.). Springer-Verlag, New York, 141-172.

Boland, J. N. and Otten, M. T., 1985. Symplectite augite: evidence for discontinuous precipitation as an exsolution mechanism in Ca-rich clinopyroxene. *Journal of Metamorphic Geology*, **3**, 13-20.

Bradley, W. H., 1929. The occurrence and origin of analcite and meerschaun beds in the Green River Formation of Utah, Colorado and Wyoming. *United States Geological Survey Professional Paper*, **158-A**, 1-7

Brown, W. L. and Parsons, I., 1981. Towards a more practical two-feldspar geothermometer. *Contributions to Mineralogy and Petrology*, **76**, 369-377.

Brown, R. E., Stevens, B. P. J., Willis, I. L., Stroud, W. J., Bradley, G.M. and Barnes, R. G., 1983. Part 3. Quartzofeldspathic rocks. In: *Rocks of the Broken Hill Block: Their classification, nature, stratigraphic distribution and origin* (edited by Stevens, B. P. J. and Stroud, W. J.). *New South Wales Geological Survey, Records*, **21(1)**, 127-226.

Burchfiel, B. C. and Royden, L. H., 1985. North-south extension within the convergent Himalayan region. *Geology*, **13**, 679-682.

Burg, J. P., Brunel, M., Gapais, D., Chen, G. M. and Liu, G. H., 1984. Deformation of leucogranites of the crystalline main central thrust sheet in southern Tibet (China). *Journal of Structural Geology*, **6**, 535-542.

Button, A. and Vos, R. G., 1977. Subtidal and intertidal clastic and carbonate sedimentation in a macrotidal environment: an example from the Lower Proterozoic of South Africa. *Sedimentary Geology*, **18**, 175-200.

Caby, R., Pecher, A. and Lefort, P., 1983. Le grand chevauchement central Himalayen: nouvelle donnees sur le metamorphism inverse a la base de la dalle du Tibet. *Revue de Geologie Dynamique et de Geographie Physique*, **24**, 89-100.

Campbell, C. V., 1971. Depositional model - upper Cretaceous Gallup beach shoreline, Ship Rock area, northwestern New Mexico. *Journal of Sedimentary Petrology*, **41**, 395-409.

Carreras, J., Estrada , A. and White, S., 1977. The effect of folding on the c-axis fabrics of a quartz mylonite. *Tectonophysics*, **39**, 3-24.

Cashman, P. H., 1990. Evidence for extensional deformation during a collisional orogeny, Rombak Window, North Norway. *Tectonics*, **9**, 859-886.

Chappell, B. W. and White, A. J. R., 1974. Two contrasting granite types. *Pacific Geology*, **8**, 173-174.

Clarke, G.L., Burg, J.P. and Wilson, C.J.L., 1986. Structural and stratigraphic constraints on the Proterozoic tectonic history of the Olary Block, South Australia. *Precambrian Research*, **34**, 107-137.

Clarke, G. L., Guiraud, M., Powell, R. and Burg, J.P., 1987. Metamorphism in the Olary Block, South Australia: compression with cooling in a Proterozoic fold belt. *Journal of Metamorphic Geology*, **5**, 291-306.

Clarke, G. L., Powell, R. and Guiraud, M., 1989. Low-pressure granulite facies metapelitic assemblages and corona textures from Mac. Robertson Land, East Antarctica: the importance of Fe_2O_3 and TiO_2 in accounting for spinel-bearing assemblages. *Journal of metamorphic Geology*, **7**, 323-335.

Clarke, G. L., Collins, W. J. and Vernon, R. H., 1990. Successive overprinting granulite facies metamorphic events in the Anmatjira Ranges, central Australia. *Journal of metamorphic Geology*, **8**, 65-88.

Clarke, G. L. and Powell, R., 1991. Proterozoic granulite facies metamorphism in the southeastern Reynolds Range, central Australia: geological context, P-T path and overprinting relationships. *Journal of metamorphic Geology*, **9**, 267-281.

Cobbold, P. R. and Quinquis, H., 1980. Development of sheath folds in shear regimes. *Journal of Structural Geology*, **2**, 119-126.

Collins, W. J. and Teyssier, C., 1989. Crustal scale ductile fault systems in the Arunta Inlier, central Australia. *Tectonophysics*, **158**, 49-66.

Collins, W. J., Williams, I. S. and Compston, W., 1991. Three short-lived granulite facies events in the Arunta Block, central Australia. *Geology*, in press

Condie, C.K., 1982. Early and Middle Proterozoic supracrustal successions and their tectonic settings. *American Journal of Science*, **282**, 341-357.

Coombs, D. S., 1965. Sedimentary analcime rocks and sodium-rich gneisses. *Mineralogical Magazine*, **34**, 144-158.

Cooper, J. A., Mortimer, G. E. and James, P. R., 1988. Rate of Arunta Inlier evolution at the eastern margin of the Entia Dome, Central Australia. *Precambrian Research*, **40/41**, 217-232.

Dalmayrac, B. and Molnar, P., 1981. Parallel thrust and normal faulting in Peru and constraints on the state of stress. *Earth Planetary Science Letters*, **55**, 473-481.

Davis, G. H. and Coney, P. J., 1979. Geological development of the Cordilleran metamorphic core complexes. *Geology*, **7**, 120-124.

Davis, G. A., Lister, G. S. and Reynolds. S. J., 1983. Interpretation of Cordilleran core complexes as evolving crustal shear zones in an extending orogen. *Abstracts with Programs, Geological Society of America*, **15**, 311.

de Raaf, J. F. M., Boersma, J. R. and van Gelder, A., 1977. Wave generated structures and sequences from a shallow-marine succession, Lower Carboniferous, County Cork, Ireland. *Sedimentology*, **24**, 451-483.

Diessel, C. F. K., 1980a. Newcastle and Tomago Coal Measures. In: *A Guide to the Sydney Basin* (edited by Herbert, C. and R. Helby, R.). *Geological Survey of New South Wales, Bulletin*, **26**, 100-114.

Diessel, C. F. K., 1980b. Excursion guide-day 1. In: *A Guide to the Sydney Basin* (edited by Herbert, C. and R. Helby, R.). *Geological Survey of New South Wales, Bulletin*, **26**, 459- 472.

Ding, P. and James, P. R., 1985. Structural evolution of the Harts Range area and its implication for the development of the Arunta Block, central Australia. *Precambrian Research*, **27**, 251-276.

Dirks, P.H.G.M., 1991. Inter-tidal and sub-tidal sedimentation during a mid-Proterozoic marine transgression, Reynolds Range Group, Arunta Block. *Australian Journal of Earth Sciences*, **37**, 409-422.

Dirks, P. H. G. M. and Wilson, C. J. L., 1990. The geological evolution of the Reynolds Range, Central Australia : Evidence for three distinct structural/metamorphic cycles. *Journal of Structural Geology*, **12**, 651-665.

Dirks, P. H. G. M. and Norman, A. R., 1991. Physical sedimentation processes on a mid-Proterozoic (1800 Ma) shelf: the Reynolds Range Group, Arunta Block, central Australia. *Precambrian Research*, submitted.

Dirks, P.H.G.M., Hand, M. and Powell, R. 1991. The P-T-deformation path for a mid-Proterozoic, low pressure terrain: the Reynolds Range, central Australia. Journal of Metamorphic Geology, in press.

Dott, R.H. and Bourgeois, J., 1982. Hummocky stratification: significance of its variable bedding sequences. *Geological Society of America Bulletin*, **93**, 663-680.

Drummond, B. J., 1988. A review of crust/upper mantle structure in the Precambrian areas of Australia and implications for Precambrian crustal evolution. *Precambrian Research*, **40/41**, 101-116.

Ellis, D.J., 1987. Origin and evolution of granulites in normal and thickened crust. *Geology*, **15**, 167-170.

Ellis, D. J. and Green, D. H., 1979. An experimental study of the effect of Ca upon garnet-clinopyroxene Fe-Mg exchange equilibria. *Contributions to Mineralogy and Petrology*, **71**, 13-22.

England, P.C., 1987. Diffuse continental deformation: length scales, rates and metamorphic evolution. In: *Tectonic Settings of Regional Metamorphism* (edited by Oxburgh, E. R., Yardley, B. W. D. and England, P. C.). The Royal Society: Cambridge University Press, London, 3-22.

England, P.C. and Thompson, A. B., 1986. Some thermal and tectonic models for crustal melting in collision zones. In: *Collision Tectonics* (edited by Coward, M. P. and Ries, A. C.). *Geological Society of London, Special Publication*, **19**, 83-84.

England, P.C. and Richardson, S.W., 1977. The influence of erosion on the mineral facies of rocks from different metamorphic environments. *Journal of the Geological Society of London* **134**, 201-213.

Etchecopar, A., 1977. A plane kinematic model of progressive deformation in a polycrystalline aggregate. *Tectonophysics* **39**, 121-139.

Etheridge, M. A., Rutland, R. W. R. and Wyborn, L. A. I., 1987. Orogenesis and tectonic processes in the Early to Middle Proterozoic of northern Australia. In: *Precambrian lithospheric evolution* (edited by Kroner, A.). *American Geophysical Union, Geodynamics Series*, **17**, 131-147.

Ewart, A. E., 1979. A review of the mineralogy and chemistry of Tertiary-Recent dacitic, latitic,rhyolitic and related salic volcanic rocks. In: *Trondhjemites, dacites and related rocks* (edited by Baker, F.). *Developments in Petrology*, **6**, 13-121. Trevier Science Publication Company, Amsterdam.

Ewart, A. E., Bryan, W. B. and Gill, J. B., 1973. Mineralogy and geochemistry of the younger volcanic islands of Tonga, SW Pacific. *Journal of Petrology*, **14**, 429-465.

Ferry, J. M. and Spear, F. S., 1978. Experimental calibration of the partitioning of Fe and Mg between biotite and garnet. *Contributions to Mineralogy and Petrology*, **66**, 113-117.

Flinn, D., 1962. On folding during three-dimensional progressive deformation. *Geological Society of London, Quarterly Journal*, **118**, 385-433.

Foden, J. D., Buick, I. S. and Mortimer, G. E. 1988. The petrology and geochemistry of granitic gneisses from the east Arunta inlier, central Australia: implications for Proterozoic crustal development. *Precambrian Research*, **40/41**, 233-259.

Forman, D. J., 1971. The Arltunga Nappe Complex, Macdonnell Ranges, N.T., Australia. *Journal of the Geological Society of Australia*, **18**, 173-182.

Forman, D. J., Milligan, E. N. and McCarthy, W. R., 1967. Regional geology and structure of the north-east margin, Amadeus Basin. *Australian Bureau Mineral Resources, Report*, **103**.

Fuhrman, M. L. and Lindsley, D. H., 1988. Ternary-feldspar modelling and thermometry. *American Mineralogist*, **73**, 201-215.

Ganguly, J. and Saxena, S. K., 1984. Mixing properties of aluminosilicate garnets: constraints from natural and experimental data, and applications to geothermo-barometry. *American Mineralogist*, **69**, 88-97.

Gass, I. G., Harris, P.G. and Holdgate, M. W., 1963. Pumice eruption in the area of the South Sandwich Islands. *Geological Magazine*, **100**, 321-330.

Gill, J. B., 1981. *Orogenic andesites and Plate tectonics*. Springer-Verlag, Berlin, Heidelberg, New York, 390 pp.

Goldsmith, J. R. and Newton, R. C., 1977. Scapolite-plagioclase stability relations at high pressures and temperatures in the system $NaAlSi_3O_8$-$CaAl_2Si_2O_8$-$CaCo_3$-$CaSO_4$. *American Mineralogist*, **62**, 1063-1081.

Goleby, B. R., Shaw, R. D., Wright, C. and Kennett, B. L. N., 1989. Geophysical evidence for "thick-skinned" crustal deformation in central Australia. *Nature*, **337**, 325-330.

Goode, A. D. T., 1978. High temperature strain rate deformation in the lower crustal Kalka Intrusion, central Australia. *Contributions to Mineralogy and Petrology*, **66**, 137-148.

Goscombe, B., 1991. Intense non-coaxial shear and the development of mega-scale sheath folds in the Arunta Block, central Australia. *Journal of Structural Geology*, **13**, 299-318.

Graham, C. M. and Powell, R., 1984. A garnet-hornblende geobarometer: calibration, testing and application to the Pelona Schist, southern California. *Journal of Metamorphic Geology*, **2**, 13-31.

Grant, J. A. and Frost, B. R., 1990. Contact metamorphism and partial melting of pelitic rocks in the Aureole of the Laramie Anorthosite complex, Morton Pass, Wyoming. *American Journal of Science*, **290**, 425-472.

Grant, J. A., 1985. Phase equilibria in partial melting of pelitic rocks. In J. R. Ashworth (ed), *Migmatites*, Blackie and Son, Glasgow, 86-144.

Green, D. H. and Ringwood, A. E., 1967. An experimental investigation of the gabbro to eclogite transformation and and its petrological applications. *Geochimica et Cosmochimica Acta*, **31**, 767-833.

Harley, S. L., 1984a. An experimental study of the partitioning of Fe and Mg between garnet and orthopyroxene. *Contributions to Mineralogy and Petrology*, **86**, 359-373.

Harley, S. L., 1984b. The solubility of alumina in orthopyroxene coexisting with garnet in FeO-MgO-Al_2O_3-SiO_2 and CaO-FeO-MgO-Al_2O_3-SiO_2. *Journal of Petrology*, **25**, 665-696.

Harley, S. L., 1989. The origin of granulites: a metamorphic perspective. *Geological Magazine*, **126**, 215-331.

Harris, N. B. W., Pearce, J. W. and Tindle, A. G., 1986. Geochemical characteristics of collision zone magmatism. In: *Collision Tectonics* (edited by Coward, M. P. and Ries, A. C.). *Geological Society Special Publication*, **19**, 67-81.

Haselton, H. T., Jr., Hovis, G. L., Hemingway, B. S. and Robie, R. A., 1983. Calorimetric investigation of the excess entropy of mixing in analbite-sanidine and solid solutions: Lack of

evidence for Na,K short range order and implications for two-feldspar thermometry. *American Mineralogist*, **68**, 398-413.

Hawthorne, F. C., 1981. Crystal chemistry of amphiboles. In: *Amphiboles and other hydrous pyriboles-mineralogy* (edited by Veblen, D. R.). *Mineralogical Society of America, Reviews in Mineralogy*, **9A**, 1-102.

Hensen, B. J., 1971. Theoretical phase relations involving cordierite and garnet in the system MgO-FeO-Al_2O_3-SiO_2. *Contributions to Mineralogy and Petrology*, **3**, 191-214.

Hensen, B. J. and Green, D. H., 1973. Experimental study of the stability of cordierite and garnet in pelitic compositions at high pressures and temperatures. III. Synthesis of experimental data and geological applications. *Contributions to Mineralogy and Petrology*, **38**, 151-166.

Heward, A.P., 1981. A review of wave dominated clastic shoreline deposits. *Earth Science Reviews*, **17**, 223-276.

Hobbs, B.E., Means, W.D. & Williams, P.F., 1976. *An outline of structural geology*. John Wiley, New York, 571 pp.

Hobbs, B. E., Archibald, N. J., Etheridge, M. A. and Wall, V. J., 1984. Tectonic history of the Broken Hill Block, Australia. In: *Precambrian Tectonics Illustrated* (edited by Kroner, A. and Greiling, R.). E. Schweizerbart'sche Verlagsbuchhandlung, Stuttgart, 353-368.

Holdaway, M. J. and Lee, S. M., 1977. Fe-Mg cordierite stability in high-grade pelitic rocks based on experimental, theoretical and natural observations. *Contributions to Mineralogy and Petrology*, **63**, 175-198.

Holland, T. J. B. and Powell, R., 1990. An internally consistent dataset with uncertainties and correlations: 4. *Journal of Metamorphic Geology*, **8**, 89-124.

Hunter, R. E., Clifton, H. E. and Phillips, R. L., 1979. Depositional processes, sedimentary structures and predicted vertical sequences in barred nearshore systems, southern Oregon coast. *Journal of Sedimentary Petrology*, **49**, 711-726.

Idnurm, M. and Giddings, J. W., 1988. Australian Precambrian polar wander: a review. *Precambrian Research*, **40/41**, 61-88.

Inman, D.L. and Nordstrom, C.E., 1971. On the tectonic and morphologic classification of coasts. *Journal of Geology*, **79**, 1-21.

Ito, K. and Kennedy, G. C., 1971. An experimental study of the basalt-garnet-granulite-eclogite transition. In: *The structure and physical properties of the earth's crust* (edited by Heacock, J. G.). American Geophysics Union, Washington, Monograph, **14**, 303-314.

Iyer, S. S., Woodford, P. J. and Wilson, A. F., 1976. Rb-Sr isotopic studies of a polymetamorphic granulite terrain, Strangways Range, central Australia. *Lithos*, **9**, 211-224.

James, P. R. and Ding, P., 1988. Caterpillar tectonics in the Harts Range area: a kinship between two sequential Proterozoic extension-collision orogenic belts within the eastern Arunta Inlier of central Australia. *Precambrian Research*, **40/41**, 199-216.

James, S. D., Pearce, J. A. and Oliver, R. A., 1987. The geochemistry of the Lower Proterozoic Willyama Complex volcanics, Broken Hill Block, New South Wales. In: *Geochemistry and mineralization of Proterozoic volcanic suites* (edited by Pharaoh, T. C., Beckinsale, R. D. and Richard, D. T.). *Geological Society of London, Special Publication*, **33**, 395-408.

Joklik, G. F., 1955. The Geology and Mica Fields of the Harts Range, central Australia. *Bureau of Mineral Resources , Australia, Bulletin* **26**.

Kerrick, D. M., Crawford, K. E. and Randazzo, A. F., 1973. Metamorphism in the roof pendants in the Sierra Nevada. *Journal of Petrology*, **14**, 301-325.

Kröner, A., 1985. Evolution of the Archaen continental crust. *Annual Reviews of Earth and Planetary Science*, **13**, 49-74.

Kohn, M. J. and Spear, F. S., 1989. Empirical calibration of geobarometers for the assemblage garnet-hornblende-plagioclase-quartz. *American Mineralogist*, **74**, 77-84.

Komar, P. D., Neudeck, R. H. and Kulm, L. D., 1972. Observations and significance of deep-water oscillating ripple marks on the Oregon continental shelf. In: *Shelf Sediment Transport* (edited by Swift, D., Duane, O. and Pilkey, O.). Dowden, Hutchinson and Ross, Stroussburg, 601-619.

Kretz, R., 1982. Transfer and exchange equilibria in a portion of the pyroxene quadrilateral as deduced from natural and experimental data. *Geochimica et Cosmochimica Acta*, **46**, 411-422.

Kretz, R., 1983. Symbols for rock-forming minerals. *American Mineralogist*, **68**, 277-279.

Krogh, E. J., 1988. The garnet-clinopyroxene Fe-Mg geothermometer: a reinterpretation of existing experimental data. *Contributions to Mineralogy and Petrology*, **99**, 44-48.

Laajoki, K. and Korkiakoski, E., 1988. The Precambrian turbidite-tempestite transition as displayed by the amphibolite-facies Puolankajärvi Formation, Finland. *Sedimentary Geology*, **58**, 195-216.

Lachenbruch, A. H., 1979. Heat flow in the Basin and Range province and thermal effects of tectonic extension. *Pure Applied Geophysics*, **117**, 34-50.

Lefort, P., 1975. Himalayas: the collided range. Present knowledge of the continental arc. *American Journal of Science*, **275A**, 1-44.

Lillie, R. J., 1985. Tectonically buried continent/ocean boundary, Ouachita Mountains, Arkansas. Geology, **13**, 18-21.

Lillie, R. J. and Yousef, M., 1986. Modern analogs for some mid-crustal reflections observed beneath collisional mountain belts. In: *Reflection seismology: the continental crust* (edited by Barazangi, M. and Brown, L.). *Geodynamics series*, **14**, 55-65. AGU, Washington D.C.

Lindsley, D. H., 1983. Pyroxene thermometry. *American Mineralogist*, **68**, 477-493.

Lister, G. S. and Davis, G. A., 1983. Development of mylonitic rocks in an intracrustal laminar flow zone, Whipple Mountains, S.E. California. *Abstracts with Programs, Geological Society of America*, **15**, 310.

Lister, G. S. and Snoke, A. W., 1984. S-C mylonites. *Journal of Structural Geology*, **6**, 617-638.

Lonker, S. W., 1981. The P-T-X relations of the cordierite garnet-sillimanite-quartz equilibrium. *American Journal of Science*, **281**, 1056-1090.

Loosveld, R. J. H. and Etheridge, M. A., 1990. A model for low-pressure facies metamorphism during crustal thickening. *Journal of Metamorphic Geology*, **8**, 257-267.

Loughnan, F. C. and Ray, A. S., 1979. The Reids Mistake Formation at Swansea Head, New South Wales. *Journal of the Geological Society of Australia*, **25**, 473-481.

Marjoribanks, R. W., 1976. Basement and cover relations on the northern margin of the Amadeus Basin, central Australia. *Tectonophysics*, **33**, 15-32.

Martin, H., Chauvel, C. and Jahn, B. M., 1983. Major and trace element geochemistry of Archean granodioritic rocks from eastern Finland. *Precambrian Research*, **14**, 753-756.

Mawer, C. K., 1980. Structural studies in the Chewings Range, Northern Territory, Australia. Ph.D thesis, Monash University, Clayton (unpublished).

Mawer, C. K., 1983. State of strain in a quartzite mylonite, central Australia. *Journal of Structural Geology*, **5**, 401-409.

McCubbin, D. G., 1982. Barrier islands and strand plains. in Sandstone depositional environments. *American Association of Petroleum Geology, memoir*, **31**, 247-279.

McKenzie, D. P., 1978. Some remarks on the development of sedimentary basins. *Earth and Planetary Science Letters*, **40**, 25-32.

Moore, A. C., 1973. Studies of igneous and tectonic textures and layering in the rocks of the Gosse Pile Intrusion, central Australia. *Journal of Petrology*, **14**, 49-79.

Morley, C. K., 1989. Extension, detachments and sedimentation in continental rifts (with particular reference to east Africa). *Tectonics*, **8**, 1175-1192.

Mortimer, G. E., Cooper, J. A. and James, P. R., 1987. U-Pb and Rb-Sr geochronology and geological evolution of the Harts Range ruby mine area of the Arunta inlier, central Australia. *Lithos*, **20**, 445-467.

Mushenko, C. M., 1985. Silicic tuffs in the Newcastle Coal Measures. Honours Thesis, Macquarie University (unpublished).

Nelson, D. R., Black, L. P. and McCulloch, M. T., 1989. Nd-Pb isotopic characteristics of the Mordor Complex, Northern Territory: Mid-Proterozoic potassic magmatism from an enriched mantle source. *Australian Journal of Earth Sciences* **36**, 541-551.

Newton, R. C. and Perkins, D., 1982. Thermodynamic calibration of geobarometers based on the assemblages garnet-plagioclase-orthopyroxene (clinopyroxene)-quartz. *American Mineralogist*, **67**, 203-222.

Nicolas, A. and Boudier, F., 1975. Kinematic interpretation of folds in alpine-type peridotites. *Tectonophysics* **25**, 233-260.

Nio, S. D., 1976. Marine transgressions as a factor in the formation of sand wave complexes. *Geol. Mijnb.*, **55**, 18-40.

Noakes, L. C., 1953. The structure of the Northern Territory in relation to mineralization. 5th Empire Mineral Congress, *"Geology of Australian ore deposits"*, 284-296.

Norman, A. R., 1989. Ultramylonite zones transecting high-grade Proterozoic rocks of the Strangways Orogenic Belt. *Geological Society of Australia, Abstracts*, **24**, 104-105.

Norman, A. R., Clarke, G. L. and Vernon, R. H., 1989. The tectonic history of the Strangways Orogenic Belt: a barometric response to late compression. *Geological Society of Australia, Abstracts*, **24**, 106-107.

Norman, A. R. and Clarke, G. L., 1990. A barometric response to late compression in the Strangways Metamorphic Complex, Arunta Block, central Australia. *Journal of Structural Geology*, **12**, 667-684.

Norman, A. R. and Flood, R. H., 1991. The geochemistry and structure of the Mount Schaber granofels: an altered quartz-analcime-calcite tephra. *Journal of Metamorphic Geology*, submitted.

Norman, A. R. and Vernon, R. H., 1991. Granulite facies, mid-crustal extension in a Proterozoic collisional orogen, Strangways Metamorphic Complex, central Australia. *Tectonophysics*, submitted.

Nøttvedt, A. and Kreisa, R. A., 1987. Model for the combined flow origin of hummocky cross-stratification. *Geology*, **15**, 357-361.

Oliver, R. L., Lawrence, R. W., Ding, P., Bowyer, D.G., Goscombe, B. D. and Sivell, W. J. 1988. Metamorphism and crustal considerations in the Harts Range and neighbouring regions, Arunta inlier, central Australia. *Precambrian Research*, **40/41**, 277-296.

Oxburgh, E. R. and Turcotte, D. L., 1970. Thermal structure of island arcs. *Geological Society of America, Bulletin*, **81**, 1665-1688.

Page, R. W., McCulloch, M. T. and Black, L. P., 1984. Isotopic record of Precambrian events in Australia. *Proceedings of the 27th International Geological Congress*, volume **5**, 25-72.

Park, R. G., 1981. Origin of horizontal structure in high-grade Archaen terrains. *Geological Society of Australia, Special Publication*, **7**, 481-490.

Passchier, C. W. and Simpson, C., 1986. Porphyroclast systems as kinematic indicators. *Journal of Structural Geology*, **8**, 831-843.

Paterson, S. R., Vernon, R. H. and Tobisch, O. T., 1989. A review of criteria for the identification of magmatic and tectonic foliations in granitoids. *Journal of Structural Geology*, **11**, 349-363.

Pearce, J. A. and Norry, M. J., 1979. Petrogenetic implications of Ti, Zr, Y, and Nb variations in volcanic rocks. *Contributions to Mineralogy and Petrology*, **69**, 33-47.

Pearce, J. A., Harris, N. B. W. and Tindle, A. G., 1984. Trace element discrimation diagrams for the tectonic interpretation of granitic rocks. *Journal of Petrology*, **25**, 956-983.

Perkins, D and Chipera, S. J., 1985. Garnet-orthopyroxene-plagioclase-quartz barometry: refinement and application to the English River subprovince and Minnesota River valley. *Contributions to Mineralogy and Petrology*, **89**, 69-80.

Phillips, G. N. and Wall, V. J. 1981. Evaluation of prograde regional metamorphic conditions: their implications for the heat source and water activity during metamorphism in the Willyama Complex, Broken Hill, Australia. *Bulletin de Mineralogie*, **104**, 801-10.

Platt. J. P. and Vissers, R. L. M., 1980. Extensional structures in anisotropic rocks. *Journal of Structural Geology*, **2**, 397-410.

Plumb, K. A., 1979. Structure and tectonic style of the Precambrian shields and platforms of north Australia. *Tectonophysics*, **58**, 291-325.

Poldervaart, A and Hess, H. H., 1951. Pyroxenes in the crystallization of basaltic magma. *Journal of Geology*, **59**, 472-489.

Powell, R. and Holland, T. J. B., 1988. An internally consistent dataset with uncertainties and correlations: 3. Applications to geobarometry, worked examples and a computer program. *Journal of metamorphic Geology*, **6**, 173-204.

Rapp, R. P., Watson, E. B. and Miller, C. F., 1991. Partial melting of amphibolite/eclogite and origin of Archean trondhjemites and tonalites. *Precambrian Research*, in press.

Ramsay, J. G., 1967. *Folding and fracturing in rocks.* McGraw and Hill, New York, 568.

Ramsay, J. G. and Graham, R. H., 1970. Strain variation in shear belts. *Canadian Journal of Earth Science*, **7**, 786-813.

Ramsay, J. G. and Huber, M. I., 1987. *The techniques of modern structural geology*. Volume 2, folds and fractures. Academic Press, London, 700.

Ratschbacher, L., Frisch, W., Neubauer, F., Schmid, S. M. and Neugebauer, J., 1989. Extension in compressional orogenic belts: The eastern Alps. *Geology*, **17**, 404-407.

Reading, H.G., 1986. *Sedimentary environments and facies*. Blackwell Scientific, Oxford, 615 pp.

Reineck, H.E. and Singh, I.B., 1972. Genesis of laminated sand and rhythmites in storm-sand layers of shelf mud. *Sedimentology*, **18**, 123-128.

Reineck, H.E. and Singh, I.B., 1980. *Depositional sedimentary environments, with reference to terrigenous clastics*. Springer, Berlin, 549 pp.

Richardson, S. W., 1968. Staurolite stability in a part of the system Fe-Al-Si-O-H. *Journal of Petrology*, **9**, 467-488.

Roep, Th. B. and Linthout, K., 1989. Precambrian storm wave-base deposits of early Proterozoic age (1.9 Ga), preserved in andalusite-cordierite-rich granofels and quartzite (Rämsberg area, Värmland, Sweden). *Sedimentary Geology*, **61**, 239-251.

Sandiford, M. and Wilson, C. J. L., 1984. The structural evolution of the Fyfe Hills-Khmara Bay region, Enderby Land, east Antarctica. *Australian Journal of Earth Sciences*, **31**, 403-426.

Sandiford, M., 1985a. The origin of retrograde shear zones in the Napier Complex: implications for the tectonic evolution of Enderby Land, Antarctica. *Journal of Structural Geology*, **7**, 477-488.

Sandiford, M., 1985b. The metamorphic evolution of granulites at Fyfe Hills: implications for Archaean crustal thickness in Enderby Land, Antarctica. *Journal of Metamorphic Geology*, **3**, 155-178.

Sandiford, M., 1989a. Horizontal structures in granulite terrains: A record of mountain building or mountain collapse? *Geology*, **17**, 449-452.

Sandiford, M. 1989b. Secular trends in the thermal evolution of metamorphic terrains. *Earth and Planetary Science Letters*, **95**, 85-96.

Sandiford, M. and Powell, R. 1986. Deep crustal metamorphism during continental extension: ancient and modern examples. *Earth and Planetary Science Letters*, **79**, 151-158.

Sandiford, M., Neall, F. B. and Powell, R. 1987. Metamorphic evolution of aluminous granulites from Labwor Hills, Uganda. *Contributions to Mineralogy and Petrology*, **95**, 217-225.

Schenk, V., 1984. Petrology of felsic granulites, metapelites, metabasics, ultramafics, and metacarbonates from southern Calabria (Italy): prograde metamorphism, uplift and cooling of a former lower crust. *Journal of Petrology*, **25**, 255-298.

Schilling, J. G., 1975. Azores mantle blob: rare earth evidence. *Earth and Planetary Science Letters*, **25**, 103-115.

Seifert, F., 1974. Stability of Sapphirine: a study of the aluminous part of the system MgO-Al_2O_3-SiO_2-H_2O. *Journal of Geology*, **82**, 173-204.

Seifert, F., 1975. Boron-free kornerupine: a high-pressure phase. *American Journal of Science*, **275**, 57-87.

Selverstone, J., 1988. Evidence for east-west crustal extension in the eastern Alps: implications for the unroofing history of the Tauern Window. *Tectonics*, **7**, 87-105.

Selverstone, J., Spear, F.S., Franz, G. and Morteani, G., 1984. High-pressure metamorphism in the SW Tauern Window, Austria: P-T paths from hornblende-kyanite-staurolite schists. *Journal of Petrology*, **25**, 501-531.

Shackleton, R. M. and Reis, A. C., 1984. The relation between regionally consistent stretching lineations and plate motions. *Journal of Structural Geology*, **6**, 111-117.

Shaw, R. D. and Langworthy, A. P., 1984. Geology of the Strangways Range region, Northern Territory. *Bureau of Mineral Resources, Australia.*. 1:100,000 geological map explanatory notes.

Shaw, R. D. and Stewart, A. J., 1975. Arunta Block - regional geology. In: *Economic Geology of Australia and Papua New Guinea* (edited by Knight, C. L.). *Australasian Institute of Mining and Metallurgy, Monograph*, **5**, 437-442.

Shaw, R. D. and Wells, A. T., 1983. Alice Springs, Northern Territory. *Bureau of Mineral Resources, Australia.*. Alice Springs 1:250,000 geological map explanatory notes.

Shaw, R.D., Langworthy, A.P., Offe, L.A., Stewart, A.J., Allen, A.R. and Senior, B.R., 1979. Geological report on 1:100,000-scale mapping the southeastern Arunta Block, Northern Territory. *Bureau Mineral Resources, Geology and Geophysics, Record* **1979/47**.

Shaw, R. D., Langworthy, A. P., Stewart, A. J., Offe, L. A., Jones, B. G., O'Donnell, I. C. and Knight, C. P., 1983. *Bureau of Mineral Resources, Australia.*. Alice Springs 1:250,000 geological map.

Shaw, R. D., Stewart, A. J. and Black, L. P., 1984a. The Arunta Inlier: a complex ensialic mobile belt in central Australia. Part 2: tectonic history. *Australian Journal of Earth Sciences*, **31**,457-484.

Shaw, R. D., Stewart, A. J. and Rickard, M. J., 1984b. Geology of the Arltunga-Harts Range region, Northern Territory. *Bureau of Mineral Resources, Australia*. 1:100,000 geological map explanatory notes.

Simpson, C and Schmid, S. M., 1983. An evaluation of criteria to deduce the sense of movement in sheared rocks. *Geological Society of America Bulletin*, **94**, 1281-1288.

Sivell, W. J. and Foden. J. D. and Lawrence, R. W., 1985. The Entire anorthositic gneiss, eastern Arunta inlier, central Australia: geochemistry and petrogenesis. *Australian Journal of Earth Sciences*, **32**, 449-465.

Sivell, W. J. and Foden. J. D., 1985. Banded amphibolites of the Harts Range meta-igneous complex, central Australia: an early Proterozoic basalt-tonalite suite. *Precambrian Research*, **28**, 223-252.

Sivell, W., J., 1988. Geochemistry of metatholeiites from the Harts Range, central Australia: implications for mantle source heterogeneity in a Proterozoic mobile belt. *Precambrian Research*, **40/41**, 261-275.

Skjernaa, L., 1989. Tubular folds and sheath folds: definitions and conceptual models for their development, with examples from the Grapesvare area, northern Sweden. *Journal of Structural Geology*, **11**, 689-703.

Soegaard K. and Eriksson, K. A., 1985. Evidence of tide, storm, and wave interaction on a Precambrian siliciclastic shelf: the 1700 M.Y. Ortega Group, New Mexico. *Journal of Sedimentary Petrology*, **55**, 672-684.

Soegaard K. and Eriksson, K. A., 1989. Origin of thick, first cycle quartz-arenite successions: evidence from the 1.7 Ga Oretga Group, northern Mexico. *Precambrian Research*, **43**, 129-141.

Spear, F. S., 1981. An experimental study of hornblende stability and compositional variability in amphibolite. *American Journal of Science*, **281**, 697-734.

Stewart, A. J., 1971. Potassium-argon dates from the Arltunga Nappe Complex, Northern Territory. *Journal of the Geological Society of Australia*, **17**, 205-211.

Stewart, A. J., 1981. Reynolds Range Region. *Australian Bureau of Mineral Resources*. 1:100,000 geological map explanatory notes.

Stewart, A. J., Offe, L. A., Glikson, A. J., Warren, R. G. and Black, L. P., 1980. Geology of the northern Arunta Block, Northern Territory. *Australian Bureau of Mineral Resources, Geology and Geophysics Record*, **1980/83**.

Stewart, A. J., Shaw, R. D. and Black, L. P., 1984. The Arunta Inlier: a complex ensialic mobile belt in central Australia. Part 1: Stratigraphy, correlations and origin. *Australian Journal of Earth Sciences*, **31**, 445-455.

Stormer, J. C., Jr, 1975. A practical two-feldspar thermometer. *American Mineralogist*, **60**, 667-674.

Stüwe, K. and Powell, R., 1989a. Metamorphic evolution of the Bunger Hills, east Antarctica: evidence for substantial post-metamorphic peak compression with minimal cooling in a Proterozoic orogenic event. *Journal of Metamorphic Geology*, **7**, 449-464.

Stüwe, K. and Powell, R., 1989b. Low-pressure granulite facies metamorphism in the Larsemann Hills area, East Antarctica; petrology and tectonic implications for the evolution of the Prydz Bay area. *Journal of metamorphic Geology*, **7**, 465-484 in press.

Sweet I.P. 1988. Early Proterozoic stream deposits: braided or meandering-evidence from central Australia, *Sedimentary Geology*, **58**, 277-293.

Tapponier, P., Lacassin, R., Leloup, P. H., Scharer, U., Zhong Dalai, Wu Haiwei, Liu Xiaohan, Ji Shaocheng, Zhang Lianshang and Zhong Jiayou, 1990. The Ailao Shan/Red River metamorphic belt: Tertiary left lateral shear between Indochina and south China. *Nature*, **343**, 431-437.

Teyssier, C., Amri, C. and Hobbs, B. E., 1988. South Arunta Block: The internal zones of a Proterozoic overthrust in central Australia. *Precambrian Research*, **40/41**, 157-173.

Thiessen, R. L. and Means, W. D., 1980. Classification of fold interference patterns: a reexamination. *Journal of Structural Geology*, **2**, 311-316.

Thompson, A.B. and Ridley, J.R., 1987. Pressure-temperature-time (P-T-t) histories of orogenic belts. *Philosophical Transactions of the Royal Society London*, **A321**, 27-45.

Turner, F. J., 1968. *Metamorphic Geology*. McGraw and Hill, 403 pp.

Vail, P. R., Mitchmum, R. M. and Thompson, S., 1977. Seismic stratigraphy and global changes in sea level, part 4: Global cycles of relative changes of sea level. In: *Seismic Stratigraphy - Applications To Hydrocarbon Exploration* (edited by Payton, C.). *American Association Petroleum Geology, Memoir*, **26**, 83-97.

Vallance. T. G., 1967. Mafic rock alteration and isochemical development of some cordierite-anthophyllite rocks. *Journal of Petrology*, **8**, 84-96.

Vernon, R. H. and Williams, P. F., 1988. Distinction between intrusive and extrusive sedimentary parentage of felsic gneisses: Examples from Broken Hill Block, N.S.W. *Australian Journal of Earth Sciences*, **35**, 379-388.

Vernon, R. H., 1974. Controls of mylonitic compositional layering during non-cataclastic ductile deformation. *Geological Magazine*, **111**, 121-123.

Vernon, R. H., Williams, V. A. and D'Arcy, W.F., 1983. Grain-size reduction and foliation development in a deformed granitoid batholith. *Tectonophysics*, **92**, 123-145.

Vernon, R.H., Clarke, G.L. and Collins, W.J., 1990. Very low-pressure granulite facies metamorphism and melting, Mt Stafford, central Australia. In: *High temperature metamorphism and crustal anatexis* (edited by Ashworth, J.R. and Brown, M.). Mineralogical Society special publication. Unwin-Hyman, London, in press.

Walker, R. G.. Duke, W. L. and Lechie, D. A., 1983. Hummocky stratification: significance of its variable bedding sequences: discussion and reply. *Geological Society of America Bulletin*, **94**, 1245-1251.

Warren, R. G., 1982. Metamorphic paragenesis in part of the Arunta Complex, Northern Territory. Ph.D. thesis, University of New South Wales (unpublished).

Warren, R. G., 1983a. Metamorphism and tectonic evolution of granulites, Arunta Block, central Australia. *Nature*, **305**, 300-303.

Warren, R. G., 1983b. Prograde and retrograde sapphirine in metamorphic rocks of the central Arunta Block, central Australia. *Bureau of Mineral Resources Journal of Australian Geology and Geophysics*, **8**, 139-145.

Warren, R. G. and Hensen, B. J., 1987. Peraluminous sapphirine from the Aileron district, Arunta Block, central Australia. *Mineralogical Magazine*, **51**, 409-415.

Warren, R. G. and Shaw, R. D., 1985. Volcanogenic Cu-Pb-Zn bodies in granulites of the central Arunta Block, central Australia. *Journal of Metamorphic Geology*, **3**, 481-499.

Warren, R. G. and Stewart, A. J., 1988. Isobaric cooling of Proterozoic high-temperature metamorphites in the northern Arunta Block, central Australia : implications for tectonic evolution. *Precambrian Research*, **40/41**, 175-198.

Warren, R. G. and Hensen, B. J., 1989. The P-T evolution of the Proterozoic Arunta Block, central Australia, and implications for tectonic evolution. In: *Evolution of Metamorphic Belts* (edited by Daly, J. S., Cliff, R. A. and Yardley, B. W. D.). *Geological Society, Special Publication*, **43**, 349-355.

Warren, R. G., Hensen, B. J. and Ryburn, R. J., 1987. Wollastonite and scapolite in Precambrian calc-silicate granulites from Australia and Antarctica. *Journal of Metamorphic Geology*, **5**, 213-223.

Waters, D.J., 1986. Metamorphic zonation and thermal history of pelitic gneisses from western Namaqualand, South Africa. *Transactions of the Geological Society of South Africa*, **89**, 97-102.

Wells, P. R. A., 1977. Pyroxene thermometry in simple and complex systems. *Contributions to Mineralogy and Petrology*, **62**, 129-139.

Wells, P. R. A., 1980. Thermal models for the magmatic accretion and subsequent metamorphism of continental crust. *Earth and Planetary Science Letters*, **46**, 253-65.

Wernicke, B., 1985. Uniform-sense normal simple-shear of the continental lithosphere. *Canadian Journal of Earth Science*, **22**, 108-125.

White, A. J. R. and Chappell, B. W., 1983. Granitoid types and their distribution in the Lachlan Fold Belt, southeastern Australia. In: *Circum-Pacific Plutonic terranes* (edited by Riddick, J. A.). *Geological Society of America, Memoir*, **159**, 21-34.

White, S. H., Burrows, S. E., Carreras, J., Shaw, N. D. and Humpreys, F. J., 1980. On mylonites in ductile shear zones. *Journal of Structural Geology*, **2**, 175-187.

Wickham, S. M. and Oxburgh, E. R., 1985. Continental rifts as a setting for regional metamorphism. *Nature*, **318**, 330-333.

Winchester, J. A. and Floyd, P. A., 1977. Geochemical distribution of different magma series and their differentiation products using immobile elements. *Chemical Geology*, **20**, 325-343.

Windley, B. F., 1985. Metamorphism and tectonics of the Himalaya. *Journal of the Geological Society of London*, **140**, 849-865.

Windrim, D. P. and McCulloch, M. T., 1986. Nd and Sr isotopic systematics of central Australian granulites: chronology of crustal development and constraints on the evolution of lower continental crust. *Contributions to Mineralogy and Petrology*, **94**, 289-303.

Windrim, D. P., 1983. Chemical and thermal evolution of Strangways granulites, central Australia. PhD thesis, The Australian National University, Canberra (unpublished).

Wood, B. J., 1974. The solubility of alumina in orthopyroxene coexisting with garnet. *Contributions to Mineralogy and Petrology*, **46**, 1-15.

Wood, B. J., 1987. Thermodynamics of multicomponent systems containing several solid solutions. In: *Thermodynamic Modelling of Geological Materials: Minerals, Fluids and Melts* (edited by Carmichael, I. S. E. and Eugster, H. P.). *Mineralogical Society of America, Reviews in Mineralogy*, **17**, 71-96.

Wood, B. J. and Banno, S., 1973. Garnet-orthopyroxene and orthopyroxene-clinopyroxene relationships in simple and complex systems. *Contributions to Mineralogy and Petrology*, **42**, 109-124.

Woodford, P. J., Mateen, A., Green, D. C. and Wilson, A. F., 1975. Ar/Ar geochronology of a high-grade polymetamorphic terrain, northeastern Strangways Range, central Australia. *Precambrian Research*, **2**, 375-396.

Wyborn, L. A. I., 1988. Petrology, geochemistry and origin of a major Australian 1840-1880 Ma felsic volcano-plutonic suite: a model for intracontinental felsic magma generation. *Precambrian Research*, **40/41**, 37-60.

Wyborn, L. A. I. and Chappell, B. W., 1983. Chemistry of the Ordovician and Silurian greywackes of the Snowy Mountains, southeastern Australia: an example of chemical evolution of sediments with time. *Chemical Geology*, **39**, 81-92.

Wyborn, L. A. I. and Page, R. W. 1983. The Proterozoic Kalkadoon and Ewen Batholiths, Mount Isa Inlier, Queensland: source, chemistry, age and metamorphism. *Bureau of Mineral Resources, Geology and Geophysics, Journal*, **8**, 53-69.

Wyborn, L. A. I., Page, R. W. and Parker, A. J., 1987. Geochemical and geochronological signatures in Australian Proterozoic igneous rocks. In: *Geochemistry and mineralization of Proterozoic volcanic suites.* (edited by Pharaoh, T. C., Beckinsale, R. D. and Richard, D. T.). *Geological Society of London, Special Publication*, **33**, 377-394.

APPENDIX AA.

Depositional history of the mid-Proterozoic (1800 Ma) Reynolds Range Group

Summary

Shallow-marine siliciclastic and carbonate deposits belonging to the 1800 Ma old Reynolds Range Group, central Australia, represent a transgressive sequence deposited on a low-gradient shelf, that was affected by long-shore currents, tidal currents, storm wave action, and fair weather wave action. The sediments comprise a 1100 m thick sequence in which three main depositional facies associations can be distinguished; (i) a near shore and inner shelf *quartz-arenite facies association* is overlain by a (ii) middle shelf *mudstone facies association* which contains lenses of (iii) a *carbonate facies association.* The quartz-arenite facies association mainly occurs along the northeast side of the range, and grades into the mudstone facies association towards the southwest. This suggests that the palaeo-shelf extended towards the southwest, which is in accordance with a concentration of southwest-directed palaeocurrent directions within the quartz-arenite facies. A sudden increase in thickness of quartz-arenite in the Mt Thomas area, suggests this area was the locus for fluvial sediment input. Vertical and lateral stratigraphic transitions between the facies associations are generally gradational, which may reflect coeval coexistence of all facies on the shelf and small, net, relative sea level changes.

The quartz-arenite facies association contains tide-influenced, bidirectional, small-scale trough cross-bedded, tabular cross-bedded and parallel-laminated sets that were deposited on the shoreface. These are generally overlain by large-scale trough and tabular cross-bedded sets, which were deposited on the inner shelf and record a southeast-directed long-shore current. Numerous truncation surfaces indicate that frequent storms eroded the shoreface and carried large volumes of sediment onto the shelf. The mudstone facies association consists of alternating mudstone beds and generally thin, sheet-like

quartz-sandstone beds that lack grading and traction structures. They represent storm-induced suspension deposits laid down on the middle shelf (inferred water depths <100 m). Longshore and tidal currents appear to have had little influence in this environment. Stromatolite bioherms, and rippled marls and grainstones constitute the carbonate facies association, which formed on the middle shelf in shallow marine areas of low siliciclastic sediment input. Ripples in storm sands throughout the mudstone facies association and a lack of turbidites, reflect the shallow depths and low-gradient of the shelf slope.

A general lack of tidal deposits and the non-barred nature of the palaeo-coastline, indicate a small tidal range (0-4 m). The unidirectional southeast-directed long-shore current, appears to have only influenced sedimentation on the inner shelf which suggests it resulted from prevailing (westerly) winds[AA].

[AA] Dirks, P. G. M. and Norman, A. R., 1991. Physical sedimentation processes on a mid-Proterozoic (1800 Ma) shelf: the Reynolds Range Group, Arunta Block, central Australia. *Precambrian Research* (submitted).

AA.1 Introduction

The late Archean and Proterozoic sedimentary record is characterized by thick sequences of quartz-arenite, interbedded with siltstone, mudstone, carbonate and bimodal volcanics, that form supracrustal successions deposited on cratonic blocks (Condie, 1982). The quartz-arenite is chemically and texturally super-mature and generally occurs in widespread sheet-like geometries, reflecting sedimentation under stable platform conditions; either in intra-cratonic settings or on a stable continental margin. Subsidence rates tend to be closely matched by terrigenous input resulting in up to 14 km thick, usually transgressive sequences, of fluviatile and shallow-marine sediments (e.g. Roep & Lindthout, 1989; Láa joki & Korkiakoski, 1988; Sweet, 1988; Blake et al., 1986; Soegaard & Eriksson, 1985; Button & Vos, 1977). An interpretation of Precambrian depositional processes is difficult because: 1) No modern examples (beyond the early Paleozoic) exist in which similar, extensive quartz-arenite sheets are deposited; 2) The basins in which such sediments accumulated reflect crustal responses to lithosphere and mantle processes that were restricted to the Precambrian (Plumb, 1979; Etheridge et al., 1987; Condie, 1982); 3) Fundamental differences in the biological, physical and chemical environment during the Precambrian resulted in unique sedimentary processes. The absence of land vegetation would have had a profound influence on erosional and depositional processes, while a lack of bioturbation aided the preservation potential of small-scale sedimentary structures. The lack of a fossil record makes the identification of sedimentary facies very difficult, especially within shallow-marine and fluviatile environments (Sweet, 1988).

Evidence presented in this appendix demonstrates how a combination of physical processes determines the distribution pattern of an essentially transgressive series of clastic and muddy facies on a shallow-marine, mid-Proterozoic, intra-cratonic shelf. The physical processes involved are: long-shore currents, bidirectional tidal currents, fair weather wave action and storm wave action. Individual facies are described and

interpreted with the use of palaeo-current directions which help determine the geometry of the palaeo-shelf and coastline.

AA.2 Regional geology

The Reynolds Range is a prominent northwest-trending range situated about 150 kilometres northwest of Alice Springs, central Australia (Fig. AA.1). The Reynolds Range forms part of the Arunta Block, which is a strongly deformed and metamorphosed mid- to early-Proterozoic craton that acted as basement to a series of mildly deformed late-Proterozoic intra-cratonic basins. Within the Arunta Block at least two episodes of sedimentation alternated with major orogenic events (Stewart et al., 1984; Shaw et al., 1984). The last depositional episode occurred between 1820 Ma and 1760 Ma (Collins et al., 1991; Dirks & Wilson, 1990) and resulted in the deposition of a sequence of mature quartz-arenite, mudstone, carbonate and felsic volcanic (Stewart et al., 1984), which are best preserved in the Reynolds Range (Fig. AA.1), where they are described as the Reynolds Range Group (Stewart et al., 1980, Dirks, 1991).

The base of the 1100 m thick Reynolds Range Group along the north side of the range, consists of conglomerate and massive quartz-arenite belonging to the Mount Thomas Quartzite (Stewart et al., 1980; Stewart 1981; Dirks, 1991), whereas to the south, calc-silicate occurs at the base (Dirks, 1991). The Mount Thomas Quartzite is overlain by the Pine Hill Formation which consists of siltstone and mudstone. Within the Pine Hill Formation, a 150 m thick lens of dolomite and mudstone, the Algamba Dolomite Member, crops out (Stewart et al., 1980; Dirks, 1991).

The Reynolds Range Group is highly deformed and metamorphosed from greenschist facies in the northwest (400°C, 4 kbar; Dirks et al. 1991) to granulite facies in the southeast (750°C, 4-5 kbar; Dirks et al., 1991; Fig. AA.1). Sedimentary structures and bed forms are generally well preserved in the quartz-arenite and interbedded siltstone, mudstone and carbonate of the greenschist facies regions. In the granulite terrain however, the sedimentological detail has largely been obliterated by recrystallization.

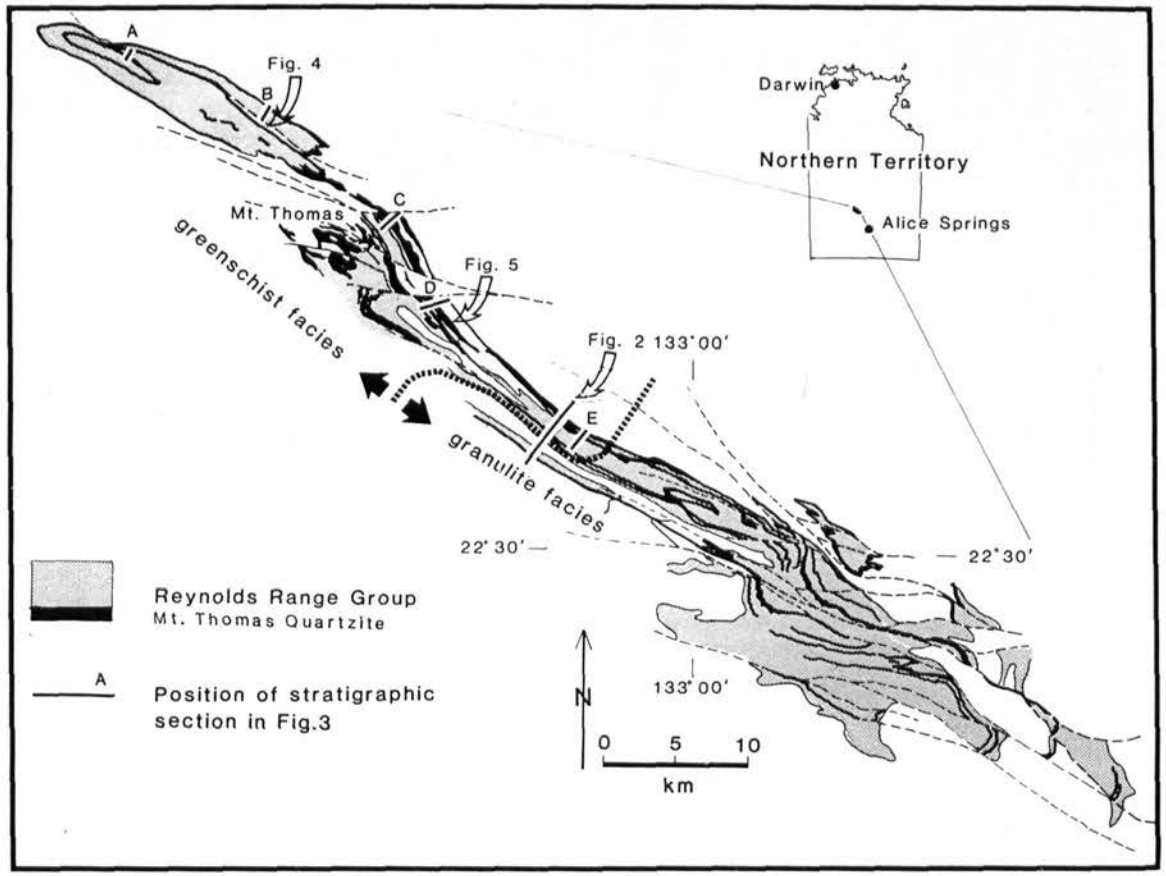

Fig. AA.1 Regional geological map of the Reynolds Range, central Australia, showing the distribution of the Reynolds Range Group and Mt Thomas quartzite from which most palaeo-current data were obtained.

In this appendix, the sedimentary facies changes are examined and the depositional history of the Reynolds Range Group is interpreted, based on observations of structures and bed forms in the greenschist facies region, where the base of the Reynolds Range Group does not contain calc-silicate. The sediments are deformed in tight, upright concentric folds. Data on bed form and sedimentary structures, were collected away from fold hinges or other structural complications, along the northeast margin of the range, where folding is least intense. Reconstruction of the palaeo-current direction was achieved by rotating the bedding planes to a horizontal position over a horizontal fold axis with an azimuth of 130°. It was assumed that folding was achieved by flexural flow, leaving the plane of the folded layer undistorted (Hobbs, et al., 1976)

AA.3 Depositional facies

The Reynolds Range Group in the northwest Reynolds Range can be divided into three depositional facies associations (Figs AA.2, AA.3) that correspond to formations described by Stewart et al. (1980) and Dirks (1990): (i) *The quartz-arenite facies association* includes fine to coarse-grained quartz-arenite with lesser amounts of conglomerate and mudstone and is characterized by traction structures and numerous reactivation surfaces. (ii) *The mudstone facies association* consists predominantly of mudstone with minor amounts of fine to medium-grained quartz-sandstone and siltstone that display structures typical of suspension deposits. In places, the mudstone facies association is interbedded with the quartz-arenite facies association (Figs AA.2, AA.3D, AA.3E). (iii) *The carbonate facies association* is made up of alternating stromatolite mats, marl and grainstone preserving wave-generated structures. The quartz-arenite facies association is most dominant along the northeast side of the range and remains very constant in thickness and appearance along the (northwest-southeast) trend of the range, but gradually thins and grades into the mudstone facies association across this trend, towards the southwest (Fig. AA.2). The mudstone facies completely envelopes laterally restricted lenses of the carbonate facies association. This facies distribution pattern suggests that the palaeo-shelf extended towards the southwest (Fig. AA.2), and that the

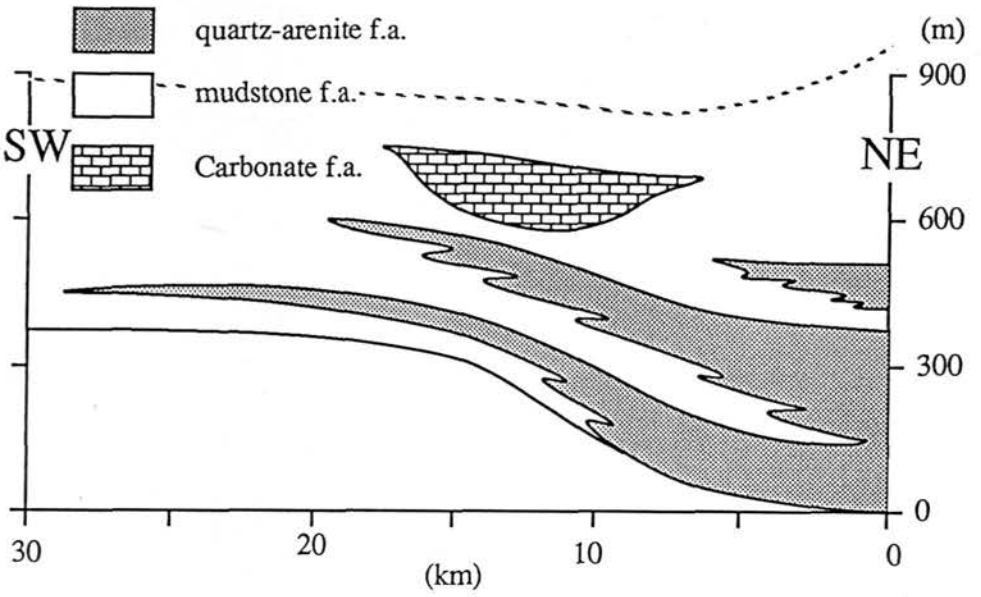

Fig. AA.2 Schematic cross section showing the spatial distribution of the three facies associations (position shown in Fig. AA.1; adapted from Dirks, 1991). The section is taken across the facies boundaries and shows a gradual northeastward and upward transition of the quartz-arenite facies association to the mudstone facies association, reflecting an overall transgression. The restored width of the palaoe-shelf is based on strain estimates across the Reynolds Range, where the lateral extend of the Reynolds Range Group was at its maximum (Dirks, 1991).

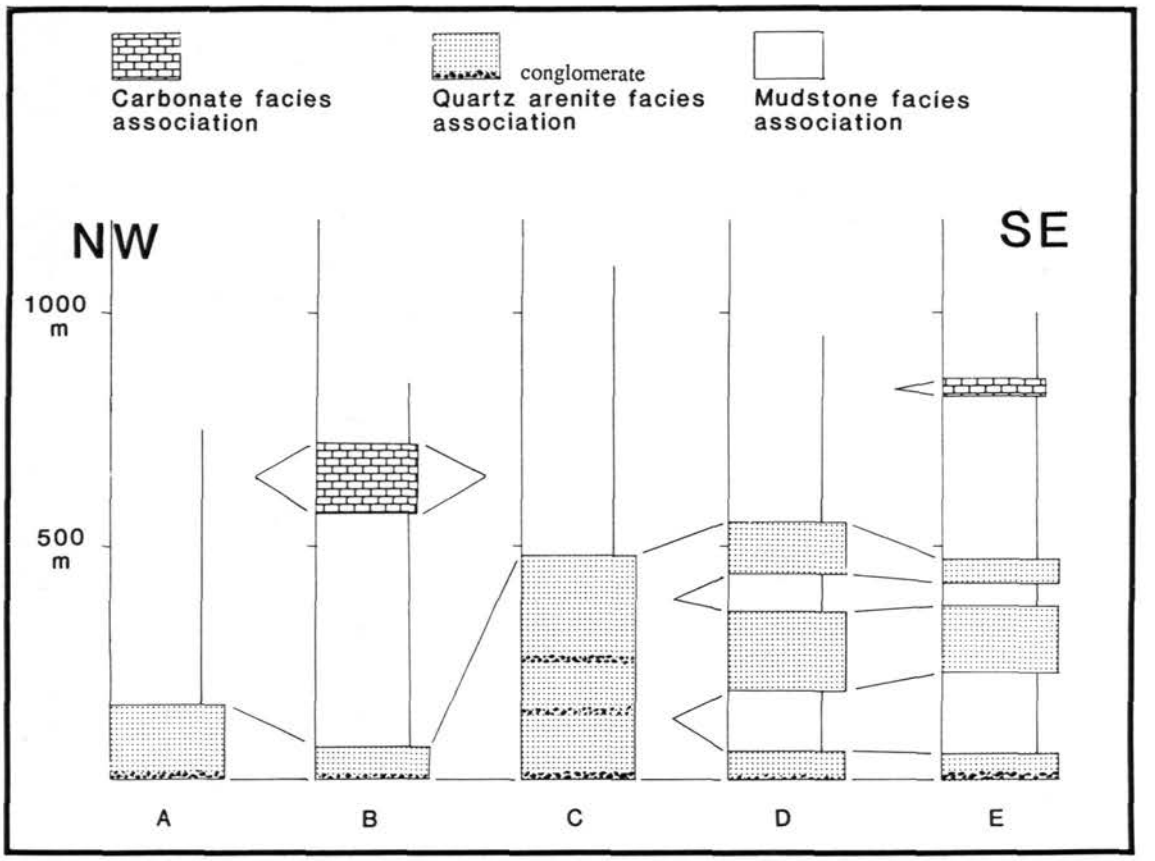

Fig.AA.3 Schematic stratigraphic columns, showing the distribution of the three facies associations along the northwestern Reynolds Range, based on stratigraphical columns presented in Dirks (1990), and indicated in fig. AA.1.

palaeo-coastline probably ran northwest-southeast, more or less parallel to the current outcrop pattern of the Reynolds Range (Figs AA.2, AA.3; Dirks, 1991).

The depositional facies associations comprise individual facies, that can be differentiated using grain size and primary sedimentary structures, which reflect the varying dominance of a particular process or sub-environment on the shelf.

AA.31 The quartz-arenite facies association

Quartz-arenite at the base of the Reynolds Range Group forms a single, massive 40-100 m thick unit in the northwest end of the range (Figs AA.3A, AA.3B, AA.4), which increases dramatically in thickness (~500 m) near Mt Thomas and farther southeast, separates in two or three units, each less than a 100 m thick, that interfinger with siltstone and mudstone (Figs AA.2, AA.3D, AA.3E, AA.5). Each unit displays an overall upward increase in grain size and bed thickness although conglomerate occurs at the base (Dirks, 1991; Figs AA.4, AA.5).

Conglomerate facies

Poorly sorted, polymict, 1-15 m thick conglomerate beds are situated directly above the unconformity at the base of the Reynolds Range Group. The conglomerate is composed of rounded to sub-angular clasts of white vein quartz (40%), siltstone and schist (40%), arkosic quartz-arenite (15%), and granite (5%). Clasts are generally pebble to cobble size and were derived from the basement schist and granite underlying the Reynolds Range Group (Dirks, 1991). Small-scale trough crossbeds record southwest-directed flow (Fig. AA.4).

Channelled trough cross-bedded facies

Channel-shaped quartz-arenite bodies occur throughout the quartz-arenite facies association but are most common towards the base (Figs AA.4 and AA.5). Channels are broad and shallow; up to 500 m wide and 10 m thick. Beds generally thin upwards and are almost entirely composed of 0.1 to 0.4 m thick sets with trough crossbeds truncated

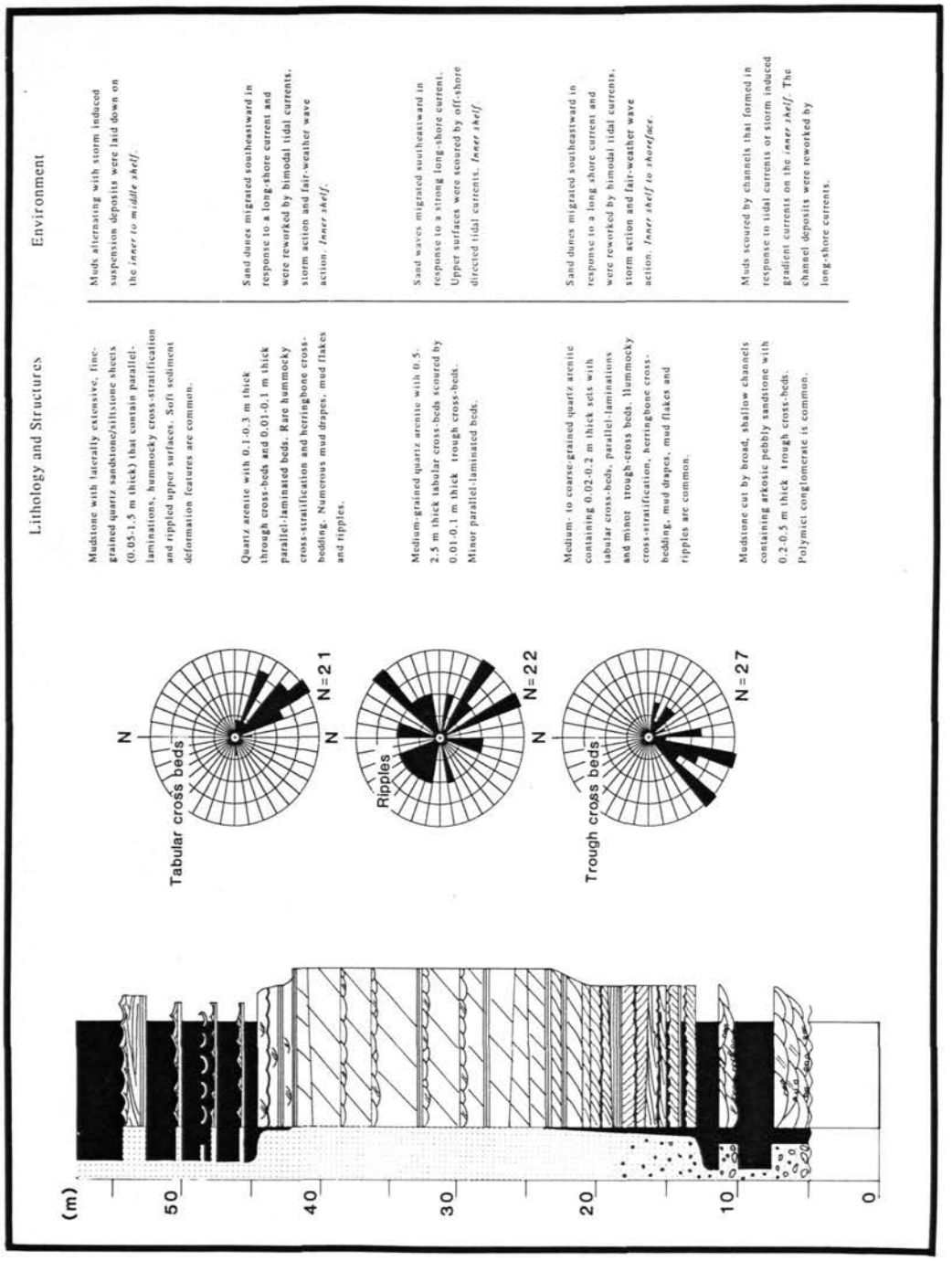

Fig. AA.4 Stratigraphic column through a transgressive sequence within the quartz-arenite facies association, northwest of Mt Thomas (Fig. AA.3B). The facies association is dominated by prominent large-scale trough and tabular cross-bedded sets. Rose diagrams indicate palaeocurrent directions.

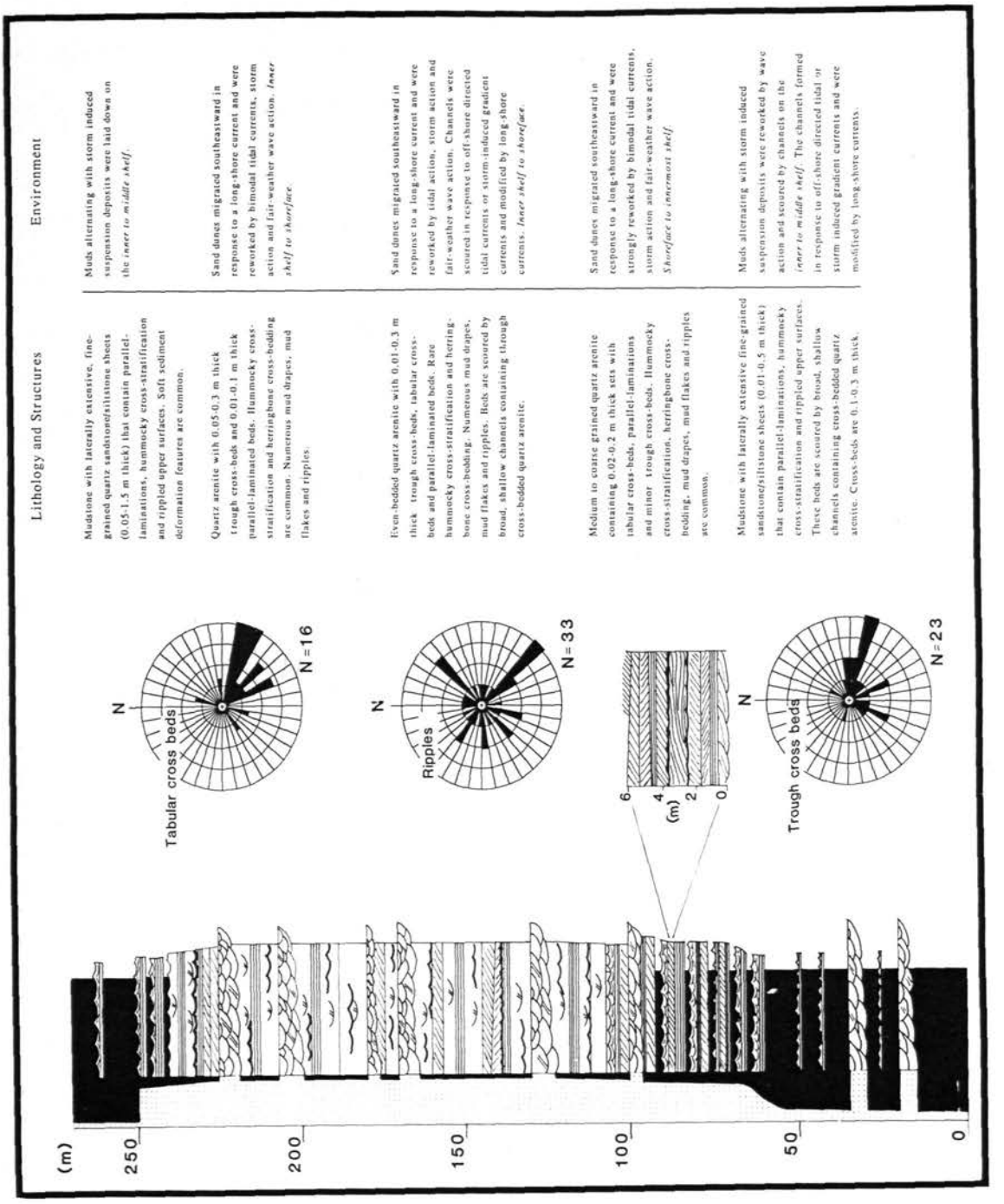

Fig. AA.5 Stratigraphic column through a transgressive sequence within the quartz-arenite facies association, southeast of Mt Thomas (Fig. AA.3D, middle quartz-arenite unit). Rose diagrams indicate palaeocurrent directions.

by numerous reactivation surfaces. The quartz-arenite is medium to coarse-grained and well sorted, and single troughs may have coarser sands and pebbles along their erosional base. Flow directions recorded in this facies are generally towards the southeast (Figs AA.5, AA.6); parallel to the facies boundaries. Southwest-northeast oriented, bidirectional flow is subordinate and is restricted to smaller trough crossbeds and locally developed herringbone crossbeds that scour the tops of larger structures.

Large-scale tabular and trough cross-bedded facies

This facies lacks mudstone and is dominant towards the centre and top of the quartz-arenite facies association (Fig. AA.4). Sets range in height from 0.2 m to 2.6 m, have tabular geometries and generally a non-erosional base. Upper surfaces may be scoured by 0.01 m to 0.15 m thick trough cross-bedded sets and separated by up to 0.2 m thick parallel-laminated beds (Fig. AA.7a). In the Mt Thomas area (Fig. AA.1), the facies contains several, up to 150 cm thick, oligomict conglomerate beds that consist of well-rounded white quartzite pebbles (< 0.8 m in diameter).

Large-scale tabular crossbeds record unidirectional flow towards the southeast, parallel to the facies boundaries (Figs AA.4, AA.6). The small-scale trough crossbeds that overlie the large cosets, generally record unidirectional southwest-directed flow, which is shown in Fig. AA.4.

Small-scale trough cross-bedded, tabular cross-bedded and parallel-laminated facies

A major component of the quartz-arenite facies association consists of small-scale trough cross-bedded, tabular cross-bedded and parallel-laminated quartz-arenite that either occurs towards the base or less commonly, throughout the facies association (Figs AA.4, AA.5).

Tabular and trough crossbeds, between 0.01 and 0.2 m thick, alternate with less than 0.1 m thick parallel-laminated beds and thin mud drapes (< 0.04 m). Low-angle cross-bedding, hummocky cross-stratification and herringbone cross-bedding are

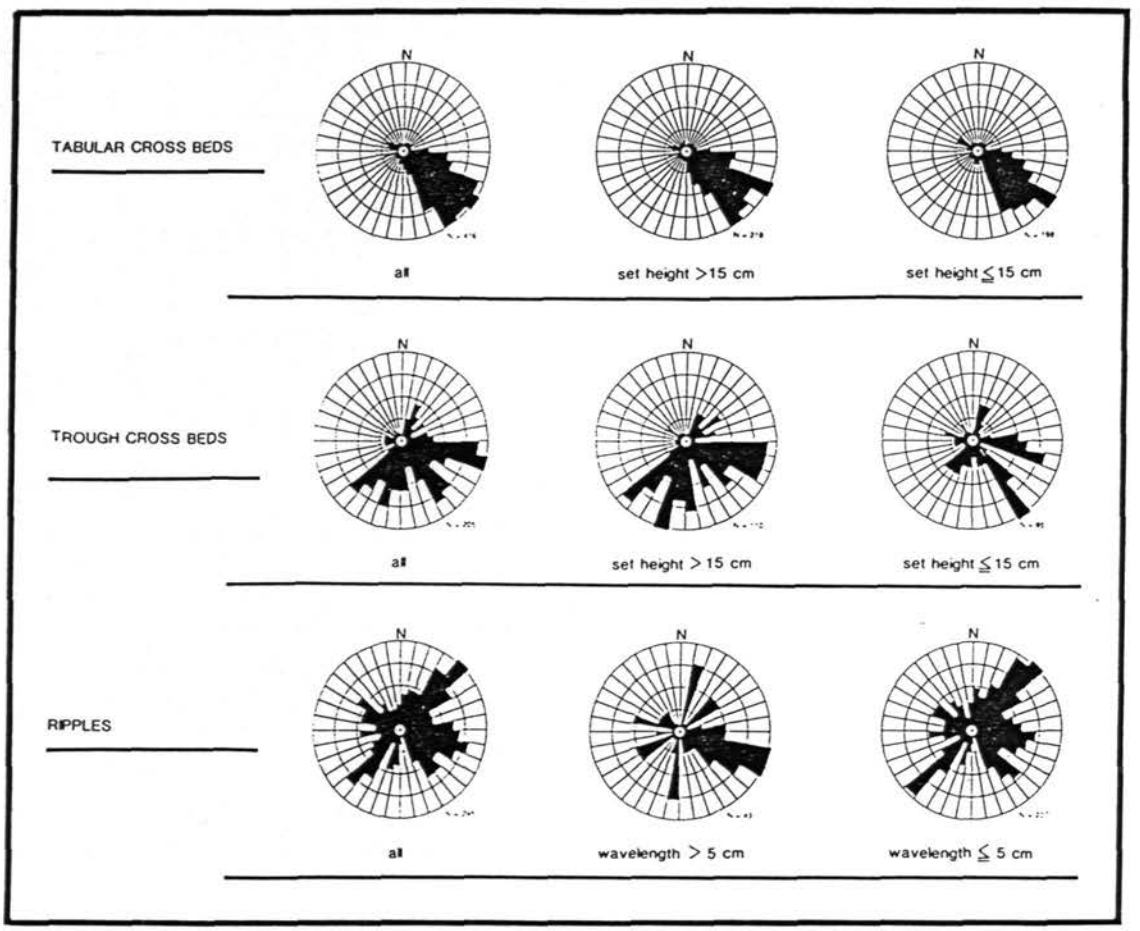

Fig. AA.6 Rose diagrams of palaeocurrent directions in the quartz-arenite facies association. Trough crossbeds, tabular crossbeds and ripples (symmetrical + asymmetrical) have been considered separately and are subdivided in large and small-scale structures.

Fig. AA.7 (a) Quartz-arenite with long-shore-directed, large-scale, tabular crossbeds. The upper coset surfaces are truncated by off-shore-directed, small-scale trough crossbeds. Note that the photo has been rotated 90° in an anticlockwise fashion, so as to bring the bedding in its original position. (photo location is towards the centre of Fig. AA.4; pencil is in top of photo)

AA.7 (b) Quartz-arenite containing parallel-laminations and herringbone cross-bedding deposited in a tide-influenced near shore environment.

AA.7 (c) Parallel-laminated and hummocky cross-stratified cosets topped by thin cross laminations in a thick storm sand deposit (photo location is towards the top of Fig. AA.4).

AA.7 (d) Loadcast and flame structures in a storm sand layer overlaying mudstone. The structures resulted from rapid suspension sedimentation on water-laden muds.

AA.7 (e) Mushroom-shaped stromatolite bioherms, draped in parallel-laminated algal mats.

AA.7 (f) Mudstone containing linsen-like grainstone lenses with a bidirectional bundled build-up typical for a high energy environment influenced by wave action. The pencil used for scale is approximately 15 cm long.

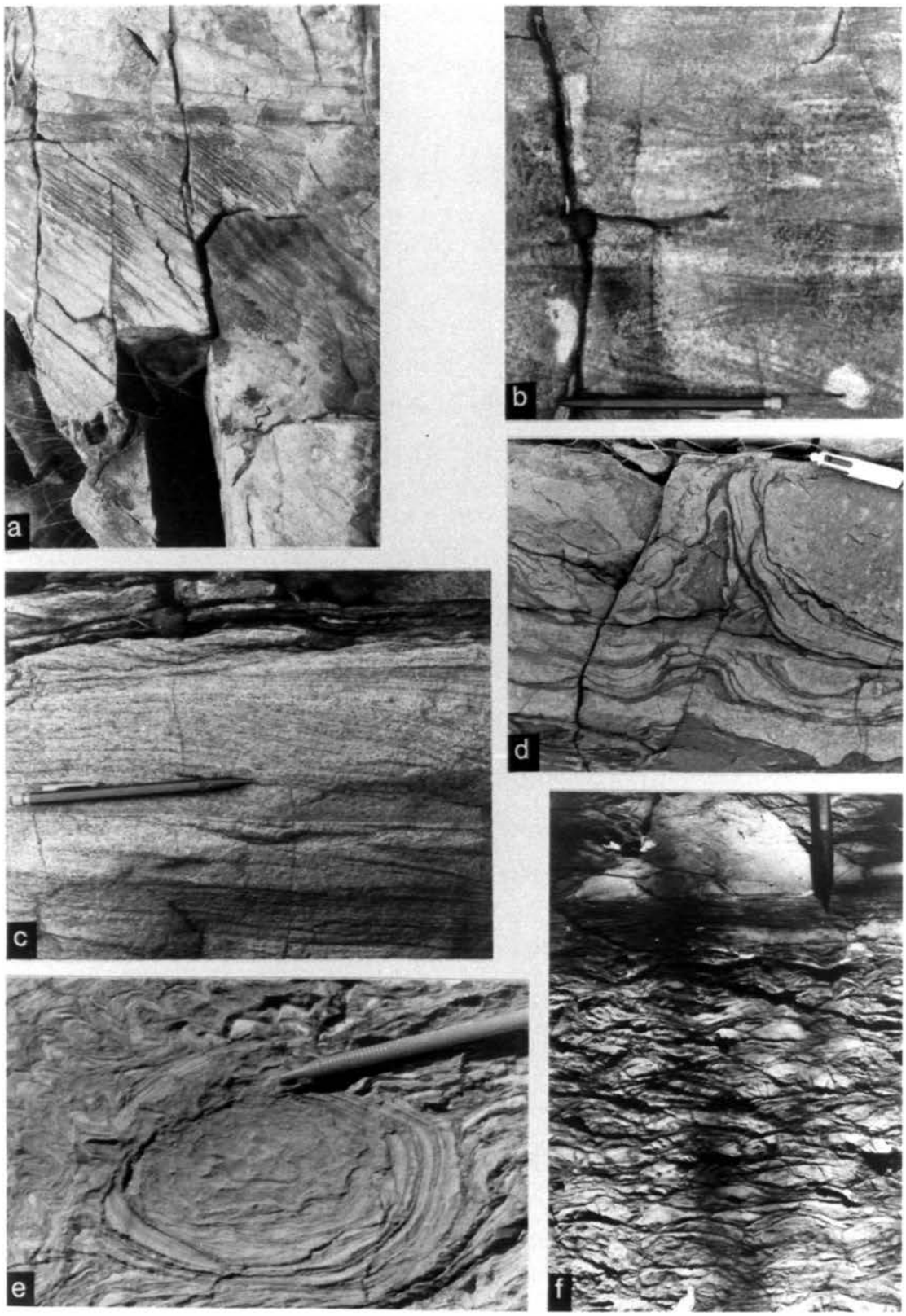
a
b
c
d
e
f

common features (Fig. AA.7b). Laterally discontinuous sets are common and display curved boundaries and numerous reactivation surfaces, accentuated by thin veneers of mud and flaser structures. The upper boundaries of all beds display ripples that are mostly symmetrical. Ripple heights are less than 5 mm and wave lengths do not exceed 5 cm. Ripple crests are straight to strongly curved and commonly bifurcated. Some bedding surfaces display interference patterns of more than one set of ripples.

Trough crossbeds in this facies record bidirectional flow towards the southwest and southeast (Fig. AA.6). Occasional herringbone crossbeds also record northeast and, to a lesser extent, northwest-directed flow. Ripples record a wide range of flow directions, dominated in smaller-scale ripples (< 5 cm; Fig. AA.6) by northeast and southwest-directed flow. Eastsoutheast-directed flow is more commonly recorded by less frequent, larger-scale ripples (> 5 cm; Figs AA.5, AA.6).

Interpretation of the quartz-arenite association

Polymict conglomerate forms a thin sheet directly above the basal unconformity and was probably deposited as continental lag in an essentially erosional environment. Reworking of the conglomerate occurred during the subsequent marine onlap. The oligomictic pebble beds that occur in the massive, cross-bedded quartz-arenites (with a marine signature, see below), may have had a fluvial origin.

The well-sorted, channelled trough cross-bedded facies display high-angle, tangential cross-stratification and probably formed from sand dunes that migrated along broad, shallow, channels (Hunter et al., 1979). As they are locally scoured by herringbone structures that record bidirectional flow, normal to the main southeast trend of the channels, it is believed they formed in a marine rather than a fluvial environment, in a direction parallel to the palaeo-coastline (= facies boundaries). The dominant southeast flow direction is therefore interpreted to result from a long-shore current.

The large-scale tabular and trough crossbeds that display a dominant southeast palaeo-flow direction, formed as a result of long-shore migrating sand waves (Campbell,

1971) in a high-energy environment. The lack of erosional, channelled bases to most of the cosets within this facies suggest that extensive dune fields migrated over a shallow inner shelf similar to the dune fields that have been described in the North Sea of the Dutch coast (Nio, 1976). Individual dunes were as high as 2 m, which indicates a minimum water depth of approximately 10 m (Allen 1982).

The small-scale trough cross-bedded, tabular cross-bedded and parallel-laminated facies contains bidirectional, northeast-southwest flow directions, (most clearly recorded by small-scale ripple marks; Fig. AA.6), and suggest deposition on the innermost shelf or shoreface, influenced by tidal activity. Flaser bedding, herringbone cross-bedding and symmetrical to near symmetrical ripples contained in this facies are all indicative of this environment (de RAA.f et al., 1977; Reineck & Singh, 1980; SoegAA.rd & Eriksson, 1985; Reading, 1986). However, a lack of subaerial structures such as desiccation cracks suggest the environment non-emergent and therefore not inter-tidal. Reactivation surfaces and mud drapes, regularly alternating with sandstone layers that predominantly record off-shore-directed flow to the southwest, indicate time-velocity asymmetry for the tidal currents with ebb-tidal currents being dominant (Fig. AA.6). Oscillation ripples in mud drapes at the top of quartz-arenite beds formed during episodes of flood-tidal quiescence and record a preferential on-shore-directed flow pattern to the northeast (small-scale ripple marks; Fig. AA.6). The tidal deposits appear to be most common towards the base of the quartz-arenite facies association (Figs AA.4, AA.5). Parallel laminations, hummocky cross-stratification and low-angle cross-bedding commonly truncate the tidal deposits and resulted from high applied bed shear stresses due to wave action (Dott & Bourgeois, 1982) or a combined flow of wave surge and unidirectional back flow (Nøttvedt & Kreisa, 1987). Alternatively, some of these structures and many of the truncation surfaces resulted from largely erosional storm surges that carried large volumes of sediment to the outer shelf (SoegAA.rd & Eriksson, 1985). Oscillation ripples and some southwest-directed, small-scale trough crossbeds on top of larger trough and tabular crossbeds reflect reworking of the long-shore dune sands by wave action and ebb-tidal traction currents.

AA.32 The mudstone facies association

The mudstone and quartz-arenite facies associations display gradational transitions in which the former either overlies (Figs AA.2, AA.3A, AA.3B, AA.3.C) or interfingers with the latter (Figs AA.2, AA.3D, AA.E). The most extensive rock type in the mudstone facies association is homogeneous mudstone. This facies is not discussed any further due to a lack of sedimentological detail.

Channelled trough cross-bedded facies

This facies occurs in close proximity to the southwest and top of the quartz-arenite facies association. Sedimentary structures are similar to those in channelled quartz-arenite in the quartz-arenite facies association. However, compared to these, bed thicknesses are generally thinner (0.05-0.3 m), and channels trend southwestwards, and are scoured in mudstone. Palaeo-flow directions recorded by small-scale ripples are typically bidirectional, northeast-southwest (across facies transitions), but medium-scale through cross beds generally record southeast directed flow (measurements were infrequent and have been included in Fig. AA.6).

Laminated siltstone-sandstone facies

Parallel laminated beds of fine- to medium-grained quartz-sandstone and siltstone make up almost the entire mudstone facies association. They display an overall fining and thinning upward away from the stratigraphic contact with the quartz-arenite association. Within 100 m of this contact, sandstone beds make up 20-50 % of the facies. Further away from the contact this proportion drops to 10-20 %. Sandstone beds vary in thickness from a few mm to 8 m and have an extremely sheet-like geometry with thicker beds being laterally continuous over 30 km.

The quartz-sandstone sheets lack an erosive base, sole marks and primary current lineations, and generally have a sharp base and rippled upper surfaces. Thin sandstone beds (< 50 mm) commonly show parallel-laminations with little internal grading, whereas

some of the thicker beds (>100 mm) exhibit a gradation from parallel-laminations at the bottom to low-angle crossbeds and hummocky cross-stratification topped by 0.01-0.1 m thick ripple sets (Fig. AA.7c). Ripples are generally near symmetrical with wave lengths of 0.02-0.1 m. Ripples are generally climbing, and ripple sets commonly contain symmetrical and asymmetrical, bidirectional bundled lenses with a chevron upbuilding (de RAA.f et al., 1977) that record flow directions along a northeast-southwest axis. Loadcasts and flame structures are common (Fig. AA.7d).

The quartz-sandstone sheets vary in thickness and bedding structures depending on their proximity to the quartz-arenite facies association. Two subfacies within the laminated siltstone-sandstone facies can be distinguished based on volume, grain size and bed thickness of the quartz-sandstone sheets. *Subfacies 1* consists of alternating mudstone and quartz-sandstone directly overlying the quartz-arenite association. Here, quartz-sandstone beds are frequent, relatively thick, coarse-grained, and invariably contain hummocky cross-stratification and ripple sets. Convolute bedding and loading structures (Fig. AA.7d) are almost entirely restricted to this subfacies. *Subfacies 2* is represented by more thinly-bedded, finer-grained quartz-sandstone and siltstone sheets, which occur further away from the quartz-arenite contact and only locally develop ripple marks and hummocky cross-stratification. The transition between the two subfacies is gradational but could be taken at a point were the sandstone sheets constitute 20% of the facies association; stratigraphically 100 m from the quartz-arenite association contact.

Interpretation of the mudstone facies association

The quartz-sandstone beds within the mudstone facies association, are dominated by parallel-laminations with minor hummocky cross-stratification and climbing symmetrical ripples, and display a general absence of scours, traction structures, high-angle cross-bedding and grading. These features indicate rapid deposition, probably from suspension due to waning high-energy wave turbulence rather than gradient driven turbidity flow (Reineck & Singh, 1972; Walker et al., 1983). The alternating mudstone-sandstone beds reflect the influence of regularly recurring storms that swept sediment

from the quartz-arenite facies association on the inner shelf and shoreface, to the middle shelf were it was deposited in widely dispersed sandstone sheets.

Quartz-sandstone sheets in subfacies 1 are common, relatively thick, coarse-grained, structured and frequently rippled, and contain convolute bedding and loading structures, all of which indicate rapid deposition above storm wave base in close proximity to the erosional source. In contrast, quartz-sandstone sheets in subfacies 1 are less frequent, thinner, finer-grained and only occasionally rippled, suggesting deposition in deeper (generally below storm wave base), more distal waters, further out on the shelf.

On-shore and off-shore-directed palaeo-currents and a lack of traction structures within the quartz-sandstone beds indicate that long-shore currents and tidal currents had little effect on the distribution of the sandstone sheets and were probably weak in the deeper portions of the shelf. Alternatively, these features reflect the time scales over which the different physical processes operated. Storm surges dropped large amounts of relatively coarse-grained sediments over a short period of time and were the main cause of water turbulence on the shelf during this period. As the storm waned, background suspension of fine-grained material resumed, influenced only by long-shore or tidal currents that would leave the relatively thick underlying storm deposits undisturbed.

Trough cross-bedded quartz-arenite that occurs in wide channels crosscutting the storm deposits, are restricted to stratigraphic positions in close proximity to the quartz-arenite facies association. This means that the channelled quartz-arenites only occurred on the inner shelf where both long-shore currents and storm currents appear to have been strong. The close association of the channelled facies containing southwest trending channels, and subfacies 1 containing an abundance of storm sheets, suggests that channels were scoured by storm-induced gradient currents. The channels were probably filled by storm or tidal sands and reworked by long-shore currents causing the predominant southeast palaeocurrent direction. Tidal flow appeared to have had little influence on these deposits. A modern example of storm-filled channels reworked by long-shore currents has been described from the North Sea, off the German Coast

(Aigner & Reineck, 1982). Geological examples are recorded in the 1700 Ma Ortega Group in New Mexico (Soegaard & Eriksson, 1985, 1989).

AA.33 The carbonate facies association

Carbonate-rich sedimentary rocks occur as lenses within the mudstone facies association 10 km to the northwest and 35 km to the southeast of Mt Thomas (Fig. AA.1, AA.2). This facies association has a maximum thickness of about 150 m (Dirks 1990).

Stromatolite facies

Stromatolite boundstone beds with a thickness of 0.1-3.0 m appear throughout the facies association. They are composed of laminated algal mats or clusters of mushroom to columnar-shaped, discrete stromatolite bioherms (Fig. AA.7e). Single bioherms are up to 1.5 m across and 0.6 m high.

Alternating grainstone-mudstone facies

Up to 30 cm thick beds of grainstone and carbonate mudstone are interbedded with the stromatolites. The grainstone beds consist of well-sorted fine- to medium-grained carbonate sands and are either massive or inter-laminated with mudstones. Structures in the thicker grainstone beds are dominated by parallel-laminations, hummocky cross-stratification and less than 1.5 cm thick unidirectional-bidirectional bundled lenses of low-angle cross-laminations. The laminated grainstone-mudstone beds display linsen structures (Fig. AA.7f) and up to 0.6 m thick sets of locally climbing symmetrical ripples with a chevron upbuilding. No palaeocurrent data are available from this facies.

Interpretation of the carbonate facies association

Stromatolite bioherms and the lack of siliciclastic detritus indicate a shallow-marine clear water environment. The fact that this facies association is restricted to lenses within the mudstone facies association suggests it formed as carbonate build-ups or reefs

on the outer shelf (Dirks, 1991). Discrete bioherms and symmetrical ripple and linsen structures indicate a dominance of fair weather wave action in this environment (de Raaf et al., 1977). Most of the grainstone resulted from oscillatory wave erosion of the bioherms and the climbing ripple structures would indicate shifting sediment loads due to wave action rather than deposition from suspension. Parallel-laminated and hummocky cross-stratified sets indicate increased bed shear stresses due to intensified wave action during storms that were largely non-erosional since truncation surfaces are lacking. All structures indicate shallow water depths, however a lack of subaerial structures suggest the environment was non-emerging.

AA.4 Depositional model

The facies that occur in the Reynolds Range Group were shaped by a complex interaction of longshore current, tidal current, fair-weather wave and storm wave action on a low gradient shelf. The depositional facies associations show gradational contacts without erosional unconformities, which suggests that they coexisted on the palaeo-shelf (Fig. AA.2). The Reynolds Range Group fines upward from conglomerate and tide-influenced sediments at the base, to quartz-arenite dominated by long-shore currents on the inner shelf, through to mudstone and storm sand deposited on the middle shelf at the top. A similar facies transition occurs laterally, along the same stratigraphic level across a number of major fold structures (wave-lengths 2-5 km), as the quartz arenite facies association dominates the northeast side of the range and the mudstone facies association the southwest (Dirks 1990). This facies change resulted from an overall northeast-directed marine transgression, interspersed with minor regressions, of a northwest-southeast stretching coastline (Fig. AA.2; Dirks 1990; see below).

The quartz-arenite facies association is composed of chemically and texturally super mature sediments that are typical of a high-energy shore line (eg. Soegaard & Eriksson 1991). Sedimentary structures are dominated by tide influenced small-scale crossbeds and long-shore current influenced channelled trough crossbeds or large-scale, non-erosional, tabular and trough crossbeds (Fig. AA.4). Storm action was erosional and

caused numerous truncation surfaces and possibly scoured channels. Relatively thin bedded, channelled and tide-influenced quartz-arenite deposited near the shoreface, may constitute the entire facies association (Fig. AA.5) within the middle or top quartz-arenite units southeast of Mt Thomas (Figs AA.1; AA.3D, AA.3E). More commonly, these deposits occur towards the base of the association and are overlain by massive quartz-arenite beds that formed on the inner shelf and record a southeast-directed long-shore current (Figs AA.3A, AA.3B, AA.3C; AA.4). The distinct upward coarsening and upward bed thickening cycles that result in the latter situation, are caused by the transgression of the inner shelf facies on to the shoreface facies. Two or three such cycles can be distinguished to the southeast of Mt Thomas (Figs AA.2, AA.3D, AA.3E). They either reflect transgressive-regressive episodes or the irregular nature of sediment supply in a continuously subsiding basin.

Going from northwest to southeast, the quartz-arenite facies association shows a sudden increase in thickness in the Mt Thomas area (Figs AA.1; AA.3B vs AA.3C) followed by a gradual thinning and interfingering with the mudstone facies association (Fig. AA.3D, AA.3E). This suggests that terrigenous input of mature sediments on to the inner shelf was centred on the Mt Thomas region. Here long-shore currents picked up the sediments and transported them southeastward. Oligomict conglomerate beds may have been deposited during major floods.

The mudstone facies association consists of alternating mudstone and quartz-sandstone beds that were deposited on the middle shelf and influenced by wave processes. The sheet-like quartz-sandstone beds lack traction features on their lower surfaces and generally display parallel laminations, hummocky cross stratifications and rippled upper surfaces. They were deposited from offshore-directed, storm-induced suspension rather than gradient-induced density currents (Reineck & Singh, 1972; Soegaard & Eriksson 1985), and show no evidence of reworking by tidal and long-shore currents. Finer-grained, less voluminous storm-sands are most frequent high in the stratigraphic sequence and in the southwest of the range, reflecting deposition further out

on the shelf. Even in the finest-grained, supposedly most distal deposits, the sheeted sandstone beds locally have rippled upper surfaces, indicating that water depth did not exceed 100-150 m (Reading, 1986) and even might have been as shallow as 60 m (Komar et al., 1972).

On raised platforms on the outer shelf, relatively free of terrigenous sediment input, stromatolite bioherms formed and carbonate sediments were deposited. The abundance of symmetrical ripple marks and stromatolite build-ups indicate very shallow water depths, close to the intertidal zone. Subaerial features such as desiccation cracks were not observed, indicating that the bioherms remained submerged. Redistribution of siliciclastic sediments by long-shore currents explains the absence of bioherms for 30 km southeast of Mt Thomas, where the fluvial sediment input occurred.

Rippled storm sands throughout the mudstone facies association and a lack of gravity current-induced deposits suggest low shelf-gradients. Therefore, any small rise in sea level would have had a major effect on the facies distribution; as has been described by Bertrand-Sarfati & Moussine-Pouchkine (1988) for Proterozoic shallow-marine sediments on the West African craton. Since the facies changes in the Reynolds Range Group are generally gradational, net relative rises in sea level and input of sediments must have been slow, which is also reflected in the super-maturity of the sediments. However, some larger-scale interbedding of arenite and mudstone certainly is present (Figs AA.2, AA.3), suggesting that a number of transgressions-regressions did take place (Dirks, 1991).

Frequently recurring storms eroded the shoreface and inner-shelf sands which were swept out on the middle shelf by possibly erosive, storm-induced gradient currents. Rapid suspension sedimentation of the sands occurred as the storms waned. Observations from the North Sea show that laminated arenites and silts deposited from turbulent suspension clouds, occur as far as 45 km from the coast, at a water depth up to 40 m (Reineck & Singh, 1972). Estimates for the width of the palaeo-shelf cropping out in the Reynolds Range are in the order of 30 km (Fig. AA.2; Dirks, 1991).

The lack of tidal inlet, tidal delta, lagoonal and backbarrier facies indicate that the palaeo-coastline was non-barred and suggest a low tidal range (0-4 m) with weak tidal currents (Heward 1981). Tidal action only affected the shoreface deposits and ebb-tidal currents appear to have been dominant. In the wide inner shelf region, fluvial sands were reworked by high-energy long-shore currents and wave action rather than tidal currents.

Long-shore currents only affected the quartz-arenite facies association in the inner-shelf regions. The large-scale cross-bedded facies shows a total lack of mud drapes and very few reactivation surfaces which suggest consistency of the flow. Long-shore flow, restricted to areas close to the shore-line is best explained by prevailing strong, (westerly) winds rather than large oscillations in tides (Heward, 1981), which is consistent with a low tidal range.

Similar deposits have been described in the 1700 Ma Ortega Group in New Mexico (Soegaa^rd & Eriksson, 1985, 1989). Soeg rd & Eriksson (1985) suggest that storm-induced gradient currents swept sand along broad channels to the middle shelf where it was deposited in large lobes.

AA.5 Tectonic Implications

Extensive deposits of inner-shelf sand, development of barrier island coasts and the shape of the shelf can be related to tectonic processes. Modern coasts can be divided into collisional, trailing edge and marginal seas (Inman and Nordstrom, 1971). A shallow, wide, low-gradient, marine shelf that existed during Reynolds Range Group times is typical of a trailing edge (Afro-type) coast or epeiric sea coast. Epeiric sea coasts occur within continents and are common during periods of high global sea level (Vail et al., 1977). However, there is an absence of modern analogues for the epi-continental seas of the Proterozoic.

Precambrian supracrustal deposits such as the Reynolds Range Group are important because they may reflect crustal responses to lithosphere and mantle processes that were restricted to the Precambrian (Plumb, 1979; Etheridge et al., 1987; Condie,

1982). Within the Lower to Mid-Proterozoic Arunta Block of central Australia at least two episodes of sedimentation alternated with large scale orogenic events (Stewart et al., 1984; Shaw et al., 1984). The Reynolds Range Group was deposited during the last depositional episode, sometime after 1820 Ma when granulite facies metamorphism affected the underlying rocks (Iyer et al., 1976; Black et al., 1983; Collins et al., 1989). U/Pb isotopic studies of zircons suggest that another granulite facies metamorphism occurred at about 1730Ma (Collins et al., 1989) affecting the Reynolds Range Group. This metamorphism was probably concomitant with the southeast-trending, upright folding that produced the macroscopic fold pattern in the Reynolds Range (Dirks and Wilson, 1990). Therefore, uplift of the underlying rocks from granulite facies conditions, deposition of the Reynolds Range Group and subsequent folding and burial to granulite facies conditions occurred over a short period of time, possibly as little as 90 million years. The lack of decompression corona textures in the underlying Lander Rock Beds (c.f. Clarke et al. 1990) testifies to extremely rapid uplift, prior to deposition of the Reynolds Range Group.

Shortening during the upright folding episode was along a northeast-southwest axis, parallel to the shelf gradient and perpendicular to the Reynolds Range Group palaeo-shoreline. Rapid uplift, erosion, basin formation, deposition and closure of the Reynolds Range Group were probably part of related tectonometamorphic processes. Basin formation may have been a consequence of lithospheric and/or crustal extension and the subsequent shortening perpendicular to the shoreline could have been a compressional response to extension.

The influx of sediment and rate of subsidence of the basin must have been high, if uplift, extension and shortening of the crust occurred over a short period of time. A high rate of sediment supply can also help maintain a relatively shallow near-shore zone and barrier bar system. A low-gradient southwest dipping shelf, a strong southeast directed long-shore current and a fluvial source to the northeast can be inferred from sedimentary structures and the distribution of facies (Dirks, 1991) in the Reynolds Range

Group. The Reynolds Range Group also probably correlates with the fluvial to shallow marine sediments of the Hatches Creek Group which outcrop to the northeast of the Arunta Block in the Tennant Creek Inlier. The Hatches Creek Group is a transgressive sequence and was probably initiated by rift-related faulting as evidenced by bimodal volcanics occurring at the base of the Group and (Black et al., 1986). These sediments were deposited between 1820Ma and 1800Ma (Blake and Page, 1988) and display similar upright folds (Black et al., 1986) to the Reynolds Range Group.

The geometry of extensional systems is important in determining the shape of a subsiding basin, amount of uplift of the surrounding highlands, erosion rates and the life of the sedimentary basin (Morley 1989). A steep boundary fault (60°-70°) with a deep depth (30km) to detachment can result in a thick sedimentary sequence and large vertical displacement compared to horizontal displacement . There would also be substantial isostatic uplift and therefore high rates of erosion. With only small amounts of horizontal displacement, the rotation of the hanging wall would produce large strains that become inefficient at depth. Consequently, the high-angle boundary fault must evolve into a shallow detachment or cease to be active (Morley, 1989). Another consequence of large rotational strains could be to initiate crustal instabilities in the hanging wall that result in the horizontal collapse or shortening of the sedimentary basin towards the footwall.

A seismic profile across the Arunta Block (Goleby et al., 1989) shows moderate-angle (50°), north-dipping, deep faults; one of which extends down to the Moho. Although these faults preserve a reverse sense of movement, it is possible that they may have developed prior to deposition of the Reynolds Range Group. Movement on these moderate-angled, deep faults together with regional simple shear extension and thermal relaxation may have initiated basin formation and influenced deposition of the Reynolds Range Group.

AA.6 Conclusions

The Reynolds Range Group represents a transgressive sequence deposited on a shallow-marine shelf that was affected by a strong long-shore current, a mainly off-shore-directed tidal current, fair weather wave and storm wave action. The facies distribution pattern and palaeo-current directions show that a low-gradient shelf extended towards the southwest. Vertical and lateral stratigraphic transitions between the facies associations are gradational implying that all facies coexisted on the shelf and relative sea level changes were small.

The quartz-arenites were deposited on the inner shelf by a fluvial system that discharged in the Mt Thomas area. Along the shoreface, the sediments were influenced by time-velocity asymmetrical tidal currents in which ebb-tidal flow alternated with tranquil periods. Long-shore currents were subordinate in this environment but were dominant on the inner shelf, where they influenced the southeastward migration of large sand wave complexes. Storms were mainly erosional on the inner shelf and carried large volumes of clastic sediment to the middle shelf where it was deposited in extensive quartz-sandstone sheets. The extreme sheet-like geometry of the storm-sands, the presence of rippled upper surfaces and lack of off-shore-directed channels and turbidites testifies to a low-gradient shelf. Long-shore currents and tidal currents had little effect on the distribution of storm sand on the middle shelf and their influence appears to have been restricted to the inner shelf and shoreface. The non-barred nature of the coast line as well as a lack of tidal inlet and delta deposits suggests a low tidal range. Shoreface deposits were locally tide-dominated, only because shelf gradients were low. Longshore currents were restricted to the inner shelf and were probably due to prevailing winds rather than tidal oscillations. Where the input of siliciclastic sediment was low, build-ups of shallow-water carbonate deposition, associated with stromatolites, formed on the middle shelf. Strong prevailing westerly winds and frequent storms would be common at mid-latitudes in the southern hemisphere. This is consistent with the interpreted Precambrian apparent polar wander path for Australia (Idnurm and Giddings, 1988).

Norman, A. R. and Clarke, G. L. (1990) A barometric response to late compression in the Strangways Metamorphic Complex, Arunta Block, central Australia, *Journal of Structural Geology* Vol. 12, NO. 5/6: 667-684.

http://dx.doi.org/10.1016/0191-8141(90)90081-9